# AN EXPERIMENTAL STUDY OF A JET-DRIVEN COMPRESSIBLE VORTEX

# AN EXPERIMENTAL STUDY OF A JET-DRIVEN, COMPRESSIBLE VORTEX

By

WILLIAM THOMAS TRICK (B.E.Sc.)

A Thesis

Submitted to the Faculty of Graduate Studies

in Partial Fulfilment of the Requirements

for the Degree

Master of Engineering

McMaster University

May 1966

MASTER OF ENGINEERING (1966) McMASTER UNIVERSITY
(Mechanical) Hamilton, ontario.

TITLE: An Experimental Study of a Jet-driven Compressible Vortex

AUTHOR: William Thomas Trick, B.E.Sc. (Western Ontario)

SUPERVISOR: Dr. J.H.T. Wade

NUMBER OF PAGES: viii , 101

SCOPE AND CONTENTS: An experimental study of the flow phenomena occurring in jet-driven vortex flows was undertaken. Two vortex chambers were constructed, one using compressed air, the other using water as the working fluid. Temperatures and total and static pressures were measured at several locations in the air-driven vortex chamber, and the wall static pressure, temperature and Mach number distributions for the vortex were presented for different exit geometries and mass flow rates. A comparison of some indicative experimental results was made with the present vortex theory.

ACKNOWLEDGEMENTS.

The author wishes to express his appreciation for the assistance given him by those people who advised and helped him in this experimental investigation. He thanks particularly Dr. J.H.T. Wade for his guidance and assistance during the past 18 months.

This project was supported by the Defense Research Board Grant, number 9552-03.

CONTENTS

LIST OF ILLUSTRATIONS

## NOMENCLATURE

| Symbol | Description | Units |
|---|---|---|
| A | Radial Reynolds number equal to $m/2\pi\mu$ | Dimensionless |
| D | Diameter of vortex cylinder | L |
| I.D. | Inside diameter | L |
| In. Hg. A. | Inches of mercury absolute pressure | $M/T^2$ L |
| L | Length of vortex cylinder | L |
| m | Rate of mass flow per unit length of vortex | M/LT |
| n | General vortex exponent | Dimensionless |
| O.D. | Outside diameter | L |
| P.S.I.G. | Pounds per square inch, gauge | $M/T^2$ L |
| Pr | Reference pressure as defined in Figure 18 | $M/T^2$ L |
| R | Radial coordinate | L |
| Rr | Reference radius as defined in Figure 18 | L |
| $V_t$ | Tangential velocity | L/T |
| Z | Coordinate in the Z-direction | L |
| $\mu$ | Absolute fluid viscosity | M/LT |
| $^oR$ | Degrees Rankine | |
| $^oF$ | Degrees Fahrenheit | |

## 1. INTRODUCTION

Recently considerable interest has been stimulated in the area of power production by the possibility of direct power conversion. Of the several methods, that of magneto-hydrodynamic* generation has been seriously studied. Already generators have been constructed and tested by several American associations**. Different geometric configurations of M.H.D. generators are possible, but the two which are most likely to be used commercially are the linear channel type, Mulleney and Dibelius(27)***, and the vortex flow type, Lewellen and Grabowsky(18). The latter type has certain advantages for small power outputs and is being considered for space power systems, as well as for less demanding applications.

This study was concerned with the hydrodynamic characteristics of a contained vortex flow, and is part of a programme leading to the construction and operation of a vortex M.H.D. generator.

* "M.H.D." will be used rather than "Magnetohydrodynamics" henceforth.

** The General Electric Co., Schenectady, New York. Avco-Everett Research Laboratories, Everett, Massachusetts.

*** Numbers in parenthesis indicate references at the end of this report.

Two test vortex generators were built for the investigations, one of plexiglass and using water as the working fluid, the other of stainless steel and using high pressure air. The two generators had similar length/diameter ratios and each used a single, two-dimensional inlet nozzle along the full length of the vortex cylinder wall. Most of the experimental work was done using the stainless steel vortex generator.

## 2. LITERATURE REVIEW

Although several types of vortex phenomenon have been observed in nature, in whirlpools and tornadoes for example, vortex flows were first investigated on a mathematical basis by Helmholtz in the mid-19th century. Lamb (28), devoted a chapter of his book to a mathematical description of the behaviour of vortex flow, incorporating the work of Helmholtz and extending it, but the theory applied to frictionless fluids, or real fluids in which the assumption of negligible viscosity could be made.

Investigations of a special type of vortex flow, produced in a "Ranque-Hilsch Vortex Tube", in which the energy separation possibilities of the fluid vortex is exploited in order to produce two streams of fluid at different total temperatures, have been reported first by Ranque (1). Hilsch (2) showed the construction of a "Vortex Tube" and outlined the optimum operating conditions, based on experimental results. Williamson and Tompkins (3), Hartnett and Eckert (4), Pengelley (5), Keyes (6), and Deissler and Perlmutter (7) all refer to some aspect of "Vortex Tube" flow, and many more reports exist, with a summary of the work from 1931 to 1953 included in Westley (8).

While the methods of instrumentation and construction of vortex generators as described in the preceding references

were useful for the present study, it was recognized that the experimental results of "Vortex-Tube" investigations could not be directly used for M.H.D. vortex generators, because of basic design differences. In general, these differences were;

(a) mass flow rate and physical size of proposed M.H.D. vortex generators was an order of magnitude greater than in "Vortex-Tubes".

(b) the flow outlets of the "Vortex-Tube" were designed to optimize the energy separation, this being of little importance in M.H.D. generators.

(c) the length/diameter ratio of "Vortex-Tubes" was of the order of ten times that of proposed M.H.D. generators.

Because of these differences, the flow in the "Vortex-Tubes" tended to decay rapidly to a "forced vortex" or "solid-body" type as a result of the smaller diameters, and due to the large length/diameter ratios, possessed a significant velocity component parallel to the axis of rotation of the vortex.

An area of work involving flows which do exhibit some of the "Vortex- Tube" type of flow is that of swirling flows as described by Gambill and Greene (9). In this type of flow, the superior heat transfer characteristics of a swirling flow in a tube, as produced by a vortex chamber at the end of the tube, resulted in a higher boiling burnout heat flux than

was possible with linear flow with equivalent pumping power. This paper gave preliminary experimental results and presented data which showed a 53% increase in the burnout heat flux, when using swirling flows. The authors suggested that swirling flows might be used in applications requiring extremely high cooling fluxes, which might occur in high power density nuclear reactors, in rocket engine nozzle throats or in space craft atmospheric re-entry problems.

Vortex flows of the type occurring in the atmosphere in tornadoes have been investigated by Long (10), (11). This type of flow was characterized by having one end of the vortex system bounded by a flat plane, the other end extending theoretically to infinity. A theoretical solution was developed by Long which he thought should be applicable to the real vortex, provided the theory was applied for distances which were quite far above the ground. Experimentally, some work has been done on measuring ground level pressure distributions, during the passage of a vortex disturbance, this work being referenced in Long's papers.

Some of the earliest experimental and theoretical work in two-dimensional viscous vortices was done by Einstein and Li (12). They investigated the velocities and surface profile which occurred in large circular tanks drained through one central exit, using water as the working fluid.

Theoretical relations for the velocities were derived for the laminar flow case, and they found their theoretical model was reasonably good for low velocities, but as the strength of the vortex increased deviations between theory and experiment were marked. Upon examination of the theoretical solution, and the experimental results for higher velocities the authors found that the tangential velocity profiles would coincide if the value of fluid viscosity was increased several times before it was used in their vortex equations, which were based on laminar assumptions. This augmented viscosity term was called the "effective vicosity", and was formed of the sum of the actual fluid viscosity and of the "virtual viscosity",which was a function of the turbulence level in the vortex. It should be noted that the maximum vortex strength* in Einstein and Li's work was quite small, of the order of $10^{-2}$ of the strength of some of the "Vortex-Tube" work, and as a result, correlations based on laminar theory, while perhaps applicable for Einstein and Li's work, would not necessarily be valid for high-strength vortex flows, as considered in the present study.

M.H.D. vortex generators and hydrodynamic studies originating from this source have been discussed by Donaldson (13), (14), (15), McCune and Donaldson (16), Lewellen (17),(18), Rosenzweig (19), (20), Rosa (21), Lengyel and Ostrach (22), Weber and Marston (29), and others. For example, a theoretical review of two-dimensional theory and a critique of the

* Vortex strength is generally defined as the velocity X radius from centre of the vortex. A typical value in Einstein and Li's work would be 5 $feet^2/sec$.

assumptions made was given by Donaldson (14). He pointed out that laminar theory did not agree at all closely with experimental values at reasonably high velocities, and concluded that the Reynolds stresses were responsible for the deviation. He developed the basic incompressible turbulent theory for the vortex, but was unable to compute actual velocity profiles because of insufficient knowledge of the mixing length distribution for the turbulent vortex, which would require experimental investigation. He concluded that this theory could properly describe the velocities in a turbulent vortex, and furthermore, that his theory would be applicable for a number of vortex situations. He again pointed out that the flow character in M.H.D. generators would certainly be turbulent.

McCune and Donaldson (16) described the tangential velocity of a vortex with an axial magnetic field interaction, using viscous two-dimensional laminar theory, but the point made by Donaldson (14), that the flow exhibits turbulent rather than laminar characteristics should be noted. Another interesting point made by Donaldson (14), was that magnetic field interaction would tend to suppress to some degree the turbulence level, and that the eddy current losses as a result of this suppression might not offset the gain in performance due to the decreased turbulence level. This remains to be shown by experiment or by a more rigorous theory.

An interesting theoretical concept, concerned with the possibility of alternating current power production directly from a vortex generator, was considered by Lengyel and Ostrach (22). The M.H.D. generator in this case was analogous to the conventional alternating current induction generator in which the rotor was replaced by the rotating fluid field. The authors assumed a potential flow velocity distribution for the zero magnetic field case and showed the effect of the interaction of a weak magnetic field on the vortex flow. The solution of the first order approximation was obtained.

Another interesting design and theoretical analysis was that presented by Weber and Marston (29). They proposed a vortex generator which used liquid metals as the working fluid, to overcome two of the foremost problems in gaseous M.H.D. generators, namely; the high temperature requirements, and the limited conductivity of gases. The possible power density of the liquid metal generator could be in the order of $10^2$ times that of a gaseous vortex generator, as shown by the authors following a simple order of magnitude analysis. A radial magnetic field was used in the design to eliminate the end losses through the conducting fluid, which would be significant when using a liquid metal and an axial magnetic field, as is proposed for gaseous vortex generators. Problems of transferring the kinetic energy of the incoming high energy fluid to the revolving fluid appeared to be difficult and would have to be solved for practical utilization of the concept.

The remainder of this literature survey is concerned with the hydrodynamics of a vortex system, and the variables which are generally unaccountable with theory. In particular they are boundary layer effects, core region phenomenon, and inlet nozzle influences.

The effect of boundary layers at the end wall, and mass flow transported by the boundary layer has been considered in several papers. A theoretical attempt at explaining the effects of the boundary layers was made by Rosenzweig (19). He defined an interaction parameter which was a ratio of the mass flow passing through the boundary layer to the total mass flow. He gave equations for circulation and stream function and showed the effect of varying the value of the interaction parameter, using an iterative technique with a computer. Anderson and Taylor (31), did extensive theoretical work on the end wall boundary layer flows, and concluded that a significant portion of the radial mass flow could pass through the boundary layer at the end wall. The flow outside the boundary layer was assumed to follow a potential vortex distribution for one solution, which the authors referred to as a "strong vortex solution". Another type, called by the authors a "weak vortex solution" was also considered, in which account was taken of the loss of mass flow from the main flow into the boundary layer. This resulted in tangential velocities lower than in the first case at a particular radius.

For one particular case, when using a L/D equal to 10, and a Reynolds number based on the tangential velocity and tube radius equal to 10 , they showed that the mass flow through a turbulent boundary layer would be as much as 300 times the mass flow required to maintain a strong laminar vortex flow. They concluded that the end wall boundary layer flow could account for the serious difference between vortex strength in experimental measurements and in laminar vortex predictions. This discrepancy between theory and experimental results had previously been assumed to result from turbulence in the main flow. Experimental workers in this field differ in their opinions as to the effect of the end wall boundary layer. Donaldson(14) stated that experimental results indicated his assumption of small sidewall boundary layers was well founded, his conclusion being based on results of axial total pressure data. On the other hand, Kendall(23) by means of apparatus which permitted matching of the end wall velocity with that of the main flow, showed that, in one particular case, this matching reduced the mass flow required to generate a given vortex strength by about a factor of three. This difference, attributed to the elimination of the boundary layer, could be much larger in other cases, It should be noted that these two authors were using flows which were not necessarily comparable, since no mention of L/D was included, and the fluid in the Kendall experiment

was water, whereas in Donaldson's it was air. Also, the strength of the Donaldson vortex was greater. Another area which has some general application to this subject is that of boundary layers on rotating discs. Gregory (24), and Binnie (25) have also studied boundary layer flow on rotating discs and cones, using water.

Another generally undefined area in vortex studies is that of the core region. Potential flow theory gives a singular point at the centre of the rotating flow, while actual fluids degenerate into a solid-body type of rotation near the centre. Two-dimensional Navier-Stokes theory may be solved if some input of information of the type or extent of the flow in the core region is included. Einstein and Li (12) assumed a uniform axial velocity across the core region and equated tangential velocities and shear stress at the outer radius of the core with that of the inner radius of the annular two-dimensional region. In gaseous vortex work, the same approach has been followed, although Pengelley (5) did not make a theoretical prediction within the core region, using as one boundary condition the tangential velocity at a rotating porous exit tube. Experimentally, it has been difficult to measure magnitudes and directions of core velocities since not only is there limited space, but more important, the interference effects of the measuring probes are serious, and in most cases indeterminate. However,

Keyes(6) obtained some static pressures and total temperatures as a result of probing from the end walls, using a disc-type vortex generator with small L/D ratio, which made somewhat easier the problem of instrumentation.

An assumption present in most of the theoretical analyses except that of Mack's(30) has been that radial heat transfer was negligible. This assumption would be reasonably well-founded, particularly in the case of a high-strength vortex, since the radial mass inflow would be quite large. Mack, however, considered the effect of radial conduction for a vortex which was driven by two rotating concentric cylinders, in which the radial inflow was necessarily zero. With these assumptions, he developed and plotted the temperature-radius relation for both the rotational and irrotational case.

Further work by Donaldson and Snedeker(30) in 1962 was involved with the parameters effecting the transition of a one-celled* to a two-celled vortex** structure. The authors found experimentally that this transition was largely a function of the ratio of a characteristic tangential

* A one-celled vortex structure is one which has unidirectional axial flow.

** A two-celled vortex structure is one which has regions of total pressure lower than that of the ambient pressure field surrounding the vortex. As a result, fluid from this pressure field may be inducted into the vortex structure, generally through the core.

velocity to a characteristic radial velocity, and that the two-celled vortex existed for values of this ratio equal to 3 or larger. Futhermore, they showed that this ratio was the dominant variable affecting the pressure and velocity distributions in a turbulent vortex and not the radial Reynolds number even though laminar theory shows this Reynolds number as the major variable. Earlier work by Donaldson, and Sullivan (13), theoretical in nature, showed the multiplicity of solutions available if the one and two-celled vortex structure possibilities were completely investigated. Theoretical tangential, radial and axial velocity profiles were shown for the several families of solutions possible for a range of radial Reynolds numbers.

An important geometric variable having a considerable influence on the flow in a vortex is that of the L/D ratio. In general this ratio has been of the order of 10 to 20 when the Ranque-Hilsch effect was investigated, and smaller, of the order of .2 to 2. when investigation of the pure vortex flow was attempted, since smaller L/D ratios provide easier instrumentation access from the end walls. An experimental investigation was carried out by Kendall (23) to provide information for M.H.D. vortex generators, in which he used L/D ratios from .78 to 2.55. Futhermore, he found that the square of the Mach number inside the exit orifice radius

increased almost linearly with the increase of L/D, and as a result concluded that the flow in his generators was certainly not two-dimensional. It should be noted that all his experimental models had flow outlet through only one end of the vortex chamber. Donaldson and Snedeker (30) investigated the effect of L/D ratio on the transition of one-celled to a two-celled vortex structure through the range of 1 to 5, and found that the transition was not largely a function of L/D, but of the tangential velocity/radial velocity ratio. Total and static pressures at the open end of their vortex chamber were shown for a range of L/D from 1 to 5, as well as the transition values of tangential velocity/radial velocity for the same range.

Entrance nozzle configurations have a significant influence on the strength of a vortex. This area of investigation has been largely experimental, although Kendall (23) compared experimental local skin friction coefficients on the vortex cylinder wall with those of turbulent flow over a flat plate and found good agreement. He did this by equating the momentum of the incoming jet with that existing just inside the wall boundary layer, following experimental determination of the velocity. Various inlets were used by Kendall, rectangular slits, various numbers of tangential circular jets, and rotating porous walls. He concluded that jet driven

vortex flow had higher turbulence levels, of the order of five percent more than with rotating porus wall inlets. This was due to wall fricton and jet flow effects, and he concluded that optimization of jet geometry should reduce the turbulence level. Keyes (6) also used different inlet jet configurations and concluded that high velocity jets were proportionally less effective in producing high strength vortices. Donaldson (14) appeared to have the most organized evaluation of nozzle entrance effects. Using apparatus with various types of inlet geometries, he conducted tests in which only the inlet configuration was varied. His experimental results showed that the main parameter effecting the strength of a vortex was the radial velocity/tangential velocity ratio, and that the larger the value of this parameter, the more closely the vortex flow approached that of the laminar case.

# 3. DESIGN CONDITIONS

## 3.1 M.H.D. Considerations

An elementary analysis of a vortex M.H.D. generator by Lewellen and Grabowsky (18) showed that the power output was proportional to the square of the inlet velocity. With this in mind, the decision was made to produce a vortex with as high an inlet velocity as possible, within the existing air supply limitations.

Initially, the hydrodynamic study was to be with unheated air, but the extension of the programme to investigate temperature distributions, effects of heat conduction, and variation of fluid properties with temperature, was foreseen. For this later investigation, the addition of an upstream air heater to produce variable stagnation temperatures would be required. Since the temperature limits for this part of the programme were not finalized, the cylinder and other parts of the apparatus which would be exposed to the high temperatures were made of stainless steels, where possible, in order to provide a reasonable resistance to corrosion at elevated temperatures.

Little has been reported on the optimum L/D ratio for a vortex generator from a M.H.D. point of view, although

Kendall (23) used values from .78 to 2.55, in his test models. In lieu of definite criterion, a condition of minimum surface area for a given enclosed volume applied to a cylindrical container, would indicate a value of L/D of the order of unity. This condition would be desirable from heat-loss considerations.

## 3.2 Hydrodynamic Considerations

In an effort to produce a vortex of as high strength as possible, the wall shear stress should be minimized, both on the ends of the vortex cylinder, and on the cylinder wall. This would result if the surfaces exposed to the flow were made as smooth as possible.

The theory which presently exists is almost entirely based on two-dimension flow assumptions, and since some analytical comparisons were planned for the experimental results obtained, attempts should be made to produce a flow which would be two-dimensional if possible, particularly in the test area. To accomplish this, a rectangular slit nozzle was used for the inlet, the nozzle extending the full length of the vortex generator. This would produce a uniform mass flow and inlet velocity per unit length of vortex at the outer

radius of the rotating flow, although three dimensional effects could be expected as the radius decreased. Also, flow would escape equally from both ends of the vortex cylinder at the end plates, since the exit geometry would be identical, this providing a degree of symmetry in the vortex flow. Flow measurements would be taken in the central part of the length of the vortex, where the two-dimensional flow would be most likely.

Vortex flow, being very difficult to monitor, due to the physical probe interaction with the fluid flow field, would require that the measuring devices be as small as possible, consistent with response time and physical strength. Since probe interaction would be generally undefinable, independent methods of flow measurement would be desirable, in order that the independent results could be compared.

## 3.3 Physical Considerations

The air supply rate, being approximately 0.3 pounds / sec. at 50 P.S.I.G., and slightly less at 100 P.S.I.G., dictated the vortex inlet nozzle throat area and inlet Mach number. The L/D ratio of the vortex cylinder would be selected after having investigated the nozzle throat fabrication difficulties, M.H.D. considerations, and the

diameters of stainless steel pipe.

Available fabrication and machining facilities would limit the surface finish of the inner surface of the cylinder, of the end discs, and of the inlet nozzle profile.

The wall thickness of the stainless steel vortex cylinder would be determined by the dimensions of commercially-available, heavy wall, stainless steel tube.

Static pressure measuring holes in the flow surfaces would be made as small as possible considering fabrication difficulties and pressure response time. The expected range would be from .010 to .028 inches diameter.

# 4. DESCRIPTION OF APPARATUS

## 4.1 Plexiglass Vortex Generator

A plexiglass vortex generator was designed and fabricated to permit investigation of low-velocity vortex flows in water. It was thought that this apparatus would provide further understanding of the boundary-layer flows at the end-wall, and give tangential velocities which might be compared with the two-dimensional laminar flow predictions of Einstein and Li's theory. The initial apparatus used water as the working fluid, which was supplied from the city mains. A special feature was the variable area slit-type inlet nozzle which made possible the production of different inlet velocities and mass flows.

The cylinder was constructed of a length of 12 inch diameter clear plexiglass tubing, approximately 12 inches in length, with a wall thickness of .250 inch. A tangential slit was made along the full length of the cylinder, and an inlet chamber, constructed by laminating plexiglass sheets of 1.00 inch thickness, was fastened to the side of the cylinder using epoxy bonding agent. A flow passage of approximately 1.00 square inch, which was milled along the inside of the inlet chamber, was connected to the inlet slit in the vortex cylinder.

Details of this apparatus are shown on Figure 1, In order to vary the slit opening, six machine screws were passed through the inlet chamber wall, with a clearance fit, and were threaded into a 12 x .50 x .50 inch strip of plexiglass which was bonded to the cylinder wall. By adjusting these six screws, and using thickness gauges, the slit could be set to any opening from 0.000 to 0.062 inches. With adjustment of the upstream pressure, and the slit opening, it was possible to change the inlet velocity, and the mass flow, thereby varying the radial and tangential Reynolds numbers.

The flow outlet was at the bottom of the cylinder, through a 3.0 inch diameter hole concentric with the cylinder axis. A ledge was provided around this hole on which aluminum inserts could be positioned. Several of these inserts were produced, with exit diameters of .250, .375, .500, and 1.00 inches, and permitted the study of the effects resulting from variation of the exit hole diameter.

## 4.2 Stainless Steel Vortex Generator

### 4.2.1 Inlet Nozzle

The need for high inlet tangential velocity dictated the use of a convergent-divergent slit nozzle. The design of the profile was undertaken by Wagstaffe (32), an Engineering Physics student at McMaster University. The specifications of this nozzle, as a result of co-ordination between Wagstaffe and the

author were as follows;

| | | |
|---|---|---|
| Pressure Ratio | = | 4.4 |
| Mass flow | = | 0.210 pounds mass/second |
| Throat dimensions | = | 6.00 x 0.0235 inches |
| Exit Mach number at design pressure ratio | = | 1.57 |
| Ambient temperature | = | $530^{0}R$ |
| Dimensions of vortex inlet | = | 6.00 x 0.0377 inches |

The divergent section of the nozzle was designed using the "Method of Characteristics" as discussed by Liepmann and Roshko (33). Since the finished profile was of the order of .070 inches long, an extension duct was added to the end in order to connect the nozzle with the vortex cylinder. A slight divergence was incorporated in this connecting duct to compensate for boundary layer growth along its length.

The entire nozzle and inlet duct was constructed of annealled brass. The convergent-divergent profile was machined using a fly-cutter type of tool bit, this tool being hand ground using an optical comparator and a scale drawing of the profile, with a 50:1 enlargement.*

The nozzle block was secured with six .250 inch diameter machine cap-screws, and .500 inch diameter polished tool steel spacers, machined to approximate length on a surface grinder. The final fitting of the spacers was done by hand with thickness gauges being used to set the throat dimension. Side plates were installed on the brass blocks, with machine screws

* See Figure 2, for a scale drawing of the profile of the nozzle against which the shape of the tool bit was compared, using the optical comparator.

and dowel pins.

The completed nozzle and duct assembly was fitted to the vortex cylinder wall, and the inner block machined in place on the vortex cylinder in order to produce the same curvature on the inner block as on the vortex cylinder wall. After machining had been completed, the surface of the vortex cylinder and the nozzle block was finished with lapping compound and a wooden mandrel, while rotating the nozzle block and cylinder assembly. A view of the assembly is shown on Figure 3.

4.2.2 Vortex Cylinder

The vortex cylinder was fabricated from a length of 8 inch nominal diameter schedule 80, type A-304 stainless steel piping. It was annealled, then finish turned on the outside, leaving the dimension of approximately 8.60 inches. The support lug for the inlet nozzle was welded on, and the opening for the nozzle assembly milled in the cylinder wall. The inside diameter was finish machined, with the nozzle block in place, then the inner surface made as smooth as possible with the use of lapping compound on a wooden mandrel. The inside finished diameter was 7.685 $\pm$ .003 inches, and possessed a surface finish of 5 to 10 micro inches, root mean square.

Overall length was 7.115 $\pm$ .020 inches, with an inside

finished length of 6.00 ± .002 inches.

Ten .250 inch diameter instrumentation holes were drilled and reamed in the cylinder wall, along its length in two rows, one on either side of the cylinder wall. The openings were situated in a plane parallel to the nozzle inlet, at 1.000 inch intervals along the length. Through these holes would be inserted flow measuring devices.

Eight equally spaced holes were drilled and tapped at each end of the cylinder, into which machine screws were inserted, to secure the end plates to the cylinder. The assembly is shown in Figure 3.

4.2.3. Vortex End Plates

Several types of end plates were fabricated and used during the test programme. The first three sets of end plates were made of plexiglass, .50 inch thick. These three pair had exit hole diameters of 1.000, 1.500, 2.000 ± .010 inches, the overall diameter of the discs being slightly less than the inner diameter of the vortex cylinder. An aluminum retaining ring was provided to hold the discs in the end of the cylinder. One of each pair of discs was fitted with a set of static pressure taps, spaced .375 ± .010 inch apart, in line along a radius of the end disc. The static holes were drilled .0215 inch diameter, from the inner surface out, to open into a larger hole tapped to 1/16 inch nominal pipe thread.

Commercially available fittings were threaded into the tapered pipe thread, and "Tygon" tubing used to attach the fittings to the appropriate pressure measuring apparatus. A photograph of a plexiglass disc is shown on Figure 4.

Two steel end plates, one of which is shown in Figure 4, were made, having exit hole diameters of 1.000 $\pm$ .002, and 1.500 $\pm$ .002 inches. In the annular area of each plate a movable disc was fitted, the surface of which was flush with that of the end plate. Near the edge of the movable disc, a hole was drilled which permitted insertion of flow measuring devices. By revolving the disc, a probe could be traversed in a circular arc across the annular area, thereby placing the probe at various radial positions in the vortex.

One pair of plate glass end plates .50 inch thick, with an exit hole of 1.000 $\pm$ .030 inch diameter, was fabricated, to permit the use of Schlieren apparatus, which was used to detect density gradients in the fluid.

## 4.3 Instrumentation

During the testing programme, three types of pressure measuring devices were used. A bourdon gauge of a standard commercial grade was used as a sensing device to indicate the range of pressures encountered in a new test run. This gauge

was not used to give quantitative results. Two precision dial manometer capsule type gauges* were available and were used to monitor the majority of the test pressures. These two gauges had ranges of 0. to 60. and of 0. to 300. inches of mercury. Twice throughout the programme, the gauges were calibrated against a mercury manometer. Precision bore U-tube manometers, being filled with triple distilled mercury were used in conjunction with Cenco steel manometer scales. The tubes had been cleaned by a standard laboratory technique prior to filling. For gauge pressures greater than 36 inches of mercury, two or more U-tubes were connected in series, this procedure being used for calibration of the capsule gauges.

The barometric pressure was measured with a temperature-corrected mercurial barometer**.

The total temperature of the supply air was monitored with a 20 gauge, Brown and Sharpe, uncalibrated copper-constantan thermocouple junction. This thermocouple was inserted through the wall of the plenum chamber which supplied the inlet nozzle, this chamber being sufficiently large to assure no compressibility effects. The thermoelectric potential, with reference to a distilled water ice-bath, was measured with a potentiometer***. Millivolt-Temperature conversions

* Wallace and Tiernan Precision Dial Manometers, Type FA-145.

** Wallace and Tiernan Precision Mercurial Manometer, Type FA-13

*** Rubicon Portable Precision Potentiometer, Type No. 2745.

were done using National Bureau of Standards values.

Temperature profiles through the vortex were taken by an iron-constantan thermocouple junction which was positioned at various radial positions. The butt-welded junction was traversed across the vortex by passing the ends through plexiglass insulators which were fitted in two diametrically located .250 inch diameter instrumentation holes in the side of the vortex. The thermocouple wire was 0.010 inch diameter, the junction being slightly larger.

During the programme, a variety of total and static pressure probes were fabricated and tested. Different configurations were required, since several probing positions were tried in an effort to locate the position which gave minimum flow disturbance. Several of these probes are shown in Figures 5, and 6.

Figure 5 shows the type of probe which was used to measure the tangential velocity profiles. This particular probe consisted of a length of .020 inch O.D., .010 inch I.D. stainless steel hypodermic tubing. The mouth of the probe shown was .150 inch from the centreline of the hypodermic tubing, being ground and etched to assure a sharp, uniform opening. On the mouth end of this probe was soldered the .015 diameter spring steel wire, this being passed diagonally through the vortex to be fastened to the traversing apparatus. The other end of the probe was tensioned with a spring or

gravity device, in order to restrain the probe against the aerodynamic drag when the system was in operation. This apparatus made possible the radial positioning of the probe, by adjustment of a screw provided with 40 threads per inch, the total range being 3.875 inches. The support wire and the hypodermic tubing passed through machined plexiglass inserts which fitted the .250 inch diameter drilled and reamed openings in the vortex cylinder wall. The hole in the plexiglass insert through which the probe passed was offset from the centreline of the insert, in order to place the mouth of the probe as close as possible to the diameter of the vortex.

Figure 5 also shows three total pressure probes used in the end plate with the adjustable disc, Figure 4. The hypodermic tubing used in these probes was 0.032 inch O.D., .020 inch I.D. In each case the probe tip was approximately .250 inch from the surface of the end plate, in order to place it outside the end wall boundary layer, the selection of this dimension being based on the experimental results obtained by Kendall (23). As will be shown later in this report, probing from the end plate using the above probes was generally unsuccesful, due to flow interference.

Probe No. 1 in Figure 6 was used for the measurement of the velocity at the exit hole of the end disc. Its dimensions were 0.020 inch O.D. and .010 inch I.D. This probe

was specially fabricated to assure that the mouth of the probe remained on the centreline of the probe support, to permit velocity direction measurements by revolution of the probe support. Probe 2 and 3 could be inserted to variable radial positions through the .250 inch holes placed through the sides of vortex cylinder.

Three types of static probes are also shown in Figure 6. The first probe was inserted from the end plate, and had a diamond airfoil cross-section. This probe could be moved in an axial direction by sliding the profiled section through a similarily shaped collet in the end wall. Probes 2 and 3 were used to check the static pressure at the exit hole in the end plate.

A method of direct velocity measurement was tried with limited success. This method used a small two-bladed paddle wheel, Figure 7, which revolved on a .375 inch O.D. high-speed ball bearing, mounted on a .125 inch diameter 16 inch long section of polished drill rod. Steel channel iron 1.5 x 2.0 inch was used to make a welded U-shaped frame, the ends of which were drilled to permit the drill rod to pass through. The rod was then placed in the vortex flow, with the paddle wheel installed at the centre of the length, and the ends of the rod passed through the steel frame. Machine nuts were run up on the threaded ends of the drill rod, and used to apply

tension. A General Radio Strobotac was used to measure the speed of the paddle wheel.

The static pressures along the length of the vortex cylinder wall were measured with ten static pressure plugs which were positioned in the .250 inch diameter instrumentation holes. A collar machined on each pressure plug butted against a milled surface on the outside of the cylinder wall, and a punch-mark on the plug aligned with a similar mark on on the vortex cylinder assured alignment when reinstalled. The end of the plug exposed to the flow was finished with a file, leaving it a few thousands of an inch proud of the inner cylinder wall, the end being finally finished with emery paper, this imparting the curvature of the wall at the same time.

A Schlieren system using two 6 inch diameter parabolic mirrors was used to check the shock structure at the exit of the inlet nozzle, the nozzle being removed from the vortex cylinder for this observation. Also, the rapid change at the vortex cylinder wall in the inlet region was investigated by Schlieren apparatus. The resulting images were taken with a 4 X 5 view camera.

# 5. Discussion of Experimental Procedure and Results.

## 5.1 Stainless Steel Vortex Chamber

### 5.1.1 Static Pressures

Pressures indicative of the true stream static pressure, were measured by several means and at various locations in the vortex chamber. The majority of the results were obtained using either static pressure holes in the end-walls of the vortex chamber, or a stagnation probe turned at 90° to the flow direction. Results obtained are shown on Figures 8, 9, 18, and 19.

Three of the plexiglass end plates, with exit hole diameters of 1.000, 1.500, and 2.000 inches were provided with static pressure holes. When these plates were installed, it was possible to measure the static pressure at the end wall at a given radius. The pressures were measured with either the dial manometer capsule gauges, or the mercury manometers, whichever was applicable. The results obtained by this method are shown in Figures 8 and 9 for the 1.000 and 2.000 inch diameter exit end plates, respectively. It was possible to rotate the plexiglass end plates with respect to the vortex chamber, and this facility enabled the measurement of static pressures at different angular positions. The distributions obtained by this method for the 0°, 90°, 180° and 270° angular

positions, ($0^{o}$ corresponded to the nozzle inlet) were identical for a constant upstream pressure. These results indicated a symmetry of flow about the geometric centre of the vortex chamber.

Static pressure plugs, one type of which is shown in Figure 6A were inserted in the ten instrumentation holes along the sides of the vortex cylinder to permit the measurement of static pressures at the cylinder wall. Only slight differences were observed in these readings at a particular location, and they appeared to be a function only of the pressure tap used, since a particular plug which initially showed a deviation would continue to show it when interchanged with an adjacent plug. The differences were quite small, of the order of .5% of the average of the absolute pressures of the other nine readings. This indicated no significant pressure gradient along the length of the vortex chamber wall which was a necessary condition although not verifying the two-dimensionality of the flow.

Several types of static pressure probes were used in the early part of the programme, during which various probing positions and probe designs were tried to find the combination resulting in the least flow disturbance. Three of these probes are shown in Figure 6B, all of which were rejected because of excessive flow disturbance.

Static pressure openings were provided in the inlet nozzle in order to initially determine its performance and to calibrate the exit plane velocity. The nozzle tests are described in the appendix, Section 10.1.

5.1.2 Total Pressures

In order to calculate the Mach Number at a particular position in the vortex it was necessary to know the local total and static pressures. To measure the total pressure, several types of probes and two probing positions were investigated, the probes being described in Section 4.3, and shown in Figures 5 and 6. As a result of initial testing, which investigated the effect of probe interference on the flow, the accuracy of positioning the probe mouth, and the convenience of traversing the probe, it was concluded that the best method was to probe from the vortex cylinder walls with the hypodermic tubing probe shown in Figure 5.

The procedure used in measuring with this probe was as follows;

1. The probe and plexiglass inserts were assembled, the probe and wire passed through two aligned instrumentation holes, and the supporting steel wire fastened to the traversing apparatus.
2. The spring tensioning device was attached to the tubing-end of the probe.

4. With the vortex flow in operation, the total pressure was measured by the dial manometers, or the mercury manometers. The stabilization time was of the order 20. seconds for a 0 to 60 reading when using the 0 to 60 range instrument. (Pressures in inches of mercury.)
5. The probe was advanced to a new radial position and the procedure repeated.

Using the total pressure data obtained in the above manner, in conjunction with static pressures from the end wall, the Mach number could be calculated assuming isentropic flow at the probe mouth. The resultant Mach numbers are shown in Figures 10 and 11 at the radial positions corresponding to the end wall pressure tap locations. Most of these profiles were obtained with the probe in the mid-plane of the vortex cylinder; however, Figure 10 shows the distribution obtained 1.000 inch from one end wall. Traverses were made up to 0.5 inch from the centreline, but the reliability of data at radii less than 1.000 inch was in doubt because of the increasing effects of probe interaction.

Several different probes were inserted through the steel end plate with the movable disc, but probe interaction was severe, particularly when the movable disc was rotated in such a way that the probe was near the vortex axis. In one case, the vortex cylinder wall static pressure decreased by 22% as a result of rotating the movable disc $180^{\circ}$, the probe initially being placed adjacent to the vortex cylinder wall. In spite

of the several designs, some of which are shown in Figure 5b, interference was present to some degree for all the tests made from this position. Thus results from these probes were not considered indicative of the true vortex conditions and were not included in the final data.

5.1.3 Temperature Measurement

A knowledge of the fluid temperature was required in order that the velocity of the flow within the vortex could be obtained. While the true total temperature could not be directly measured by the apparatus shown in Figure 5a, it could be calculated knowing the Mach number at the same point and using certain empirical relations as presented by Simmons (37) which dealt with recovery factors for butt-welded thermocouples. The following technique was used to obtain the effective or adiabatic temperature of the thermocouple junction,

1. The thermocouple junction, the plexiglass inserts and the thermocouple wire were passed through two aligned instrumentation holes, and one end of the thermocouple was fastened to, but insulated from, the traversing apparatus.
2. The free end was fastened to, but insulated from, the tensioning device.
3. The cold junction was formed outside the vortex cylinder, and immersed in a distilled water ice-bath, which served as a reference.
4. The hot junction was brought up flush with the vortex cylinder wall, by means of the traversing

device, and the position of the micrometer screw noted.

5. The resultant thermoelectric potential was measured with a potentiometer.
6. The hot junction was advanced to the next radial position and the procedure repeated.

Some typical thermocouple effective temperature data are shown in Figure 12. It can be seen that the effective temperature is relatively constant for most of the vortex region, the temperature difference being of the order of $5^{o}$ to $10^{o}$ Fahrenheit. Since the effective temperature is very nearly equal to the total temperature, it is possible to conclude that the total temperature itself is approximately constant through the vortex. A more detailed analysis of the errors due to the uncalibrated thermocouple, and the empirical effective-total temperature relationship is included in Section 7.

### 5.1.4 Direct Velocity Measurement

In order to have an independent means of measurement of the tangential velocity, several small paddle-wheels were designed and built, one of which is shown in Figure 7. The apparatus was used by positioning the wheel in the centre of the vortex flow, at the appropriate axial position, and observing the velocity of the paddle-wheel with an electronic strobotac. As would be expected the speed of the wheels was quite high, particularly for those with small radii, and the

resulting centrifugal force destroyed several of them. This speed limitation made it necessary to construct paddle-wheels with a minimum radius of approximately 2 inches, thus limiting the range of applicability of this type of testing. This restriction was particularly unfortunate since the region within the 2 inch radius could not easily be explored with the other methods discussed. Since speeds of the order of 25,000 R.P.M. were measured, problems of mechanical unbalance and structural failure caused considerable concern. Results of one run are shown in Figure 13, with the point of failure of the paddle-wheel noted. A value obtained by this method from the data on Figure 13 was compared to results measured by the stagnation probe method mentioned previously and the two values found to correspond within 20%.

Preliminary results were also obtained using the paddle-wheel at various axial positions which tended to indicate that the flow was two-dimensional.

It was felt that this method of velocity measurement could be used if the mechanical problems were solved since, it was quite convenient to use, possessed small system inertia, appeared to interfere very little with the flow situation, and made extremely easy the measurement of velocities at various axial positions.

5.1.5 Schlieren Equipment

Schlieren equipment was used in two investigations in this thesis. The first was for investigation of the flow from the inlet nozzle, when removed from the cylinder, the second was for investigation of the flow at its immediate entrance to the vortex cylinder.

The results of the first investigation are described in the appendix, Section 10.1, and Figure 20 shows two photographs taken during this study.

The third photograph in Figure 20 shows the Schlieren images resulting from the light beam passing through the vortex cylinder in the vicinity of the flow inlet. The film used was of A.S.A. rating 400, using an aperture of F-4.5 and an approximate time exposure of 5 seconds. The light area immediately in the vicinity of the inlet nozzle represents the pressure change due to the wall shear stress occurring when the jet first impinges on the cylinder wall. It also shows that this initial pressure loss is a local effect, occurring in approximately the first 30 degrees after the point of injection.

5.1.6 Miscellaneous Investigations and Observations

During operation of the vortex generator, at some combinations of pressure and exit diameters, the system was observed to oscillate between two bi-stable states. The periods

of oscillation were random, but were generally of 10. to 50. seconds. An oscillation could sometimes be induced by disturbing the flow external to one of the exit holes, suggesting that the fluctuation was due to the vortex structure changing from a one-celled to a two-celled type, or vice versa. As a result an investigation of the exit hole velocities was made. At high upstream pressures, one state was stable, and for this, a velocity map was produced, which is shown in Figure 14. This structure is certainly two-celled. It was not possible to measure a one-celled profile for the range of pressures in the bi-stable region, since the measuring probe (Figure 6a-1) induced the two-celled type.

When using the 1.000 inch diameter exits and high upstream pressures, the central core region filled with a white cloud of condensed water vapour. This phenomenon did not occur at upstream pressures which were low enough to cause the bi-stable state mentioned above. The vortex generator, when in operation, was accompanied by a high noise level, and on several occasions this was measured and found to be of the order of 135 to 145 decibels. During the programme porous exit tubes had been fabricated and inserted in the core region, and the noise level with these tubes inserted was considerably reduced. Also, two tubes approximately two feet in length had been placed outside the exit holes as part of the investigation with the bi-stable states, and their presence also reduced the noise level.

## 5.2 Plexiglass Vortex Generator

Only preliminary work was carried out using this generator. Dye injection was used at the free surface of the vortex, and the core so defined was photographed both with still and cine cameras.

From the photograph of the surface profile shown in Figure 15, the tangential velocity at the surface was calculated using a method as described in the appendix, Section 10.3, the resulting values being shown in Figure 16. The ideal-flow type characteristic of increasing velocity at decreasing radius is obvious from Figure 16.

# 6. THEORETICAL WORK AND COMPARISONS WITH EXPERIMENTAL RESULTS

Since a considerable amount of work has been done on the theoretical description of vortex flows, it was thought valuable to compare the experimental results of this study to the various theoretical models. Some of the theoretical work has been described in general terms in section 2 of this report, however, the more important theoretical models, and the assumptions made by the authors involved will be reviewed in more detail in this section, and compared to experimental results where applicable.

## 6.1 Ideal or Inviscid Theory

Helmholtz, referred to in Lamb (28), for example, was responsible for the first mathematical description of a fluid vortex, when he imposed the condition of conservation of angular momentum on a fluid system. This flow is simply described by;

$$V_t R = \text{Constant.}$$

The equation is valid for positive values of the constant and values of R greater than zero. Since ideal flow theory assumes a frictionless, incompressible, two-dimensional fluid field, it is somewhat restricted when applied to a real fluid vortex, because of the inability to account for the energy

degradation due to fluid viscosity. As a result, the ideal flow theory predicts vortex tangential velocities higher than experimentally measured. Figure 17 shows the ideal theory predictions compared to some experimental data, with the ideal flow theory referenced to the experimental inlet condition. It should be noticed that the experimental velocities exhibit the same trend as the theoretical predictions, however, the discrepancy increases as the radius decreases.

## 6.2 Forced or Solid-Body Type Flow

Solid-body flow, as the name implies, is that type of flow which would be observed with liquids having infinite viscosity. It is characterized by the absence of motion between adjacent fluid particles, and is mathematically described by

$$\frac{V_t}{R} = \text{Constant}$$

This equation is valid for positive values of the constant and all positive values of R. Experimentally, most vortex flows show this characteristic type of velocity distribution in the core region. Since the flow only occurs for the limiting case of infinite viscosity or zero radial

inflow, comparisons between experiment and theoretical predictions show the former larger than the latter, although the discrepancy decreases as the centre of the rotating flow is approached. The difficulties in experimentally measuring tangential velocities in the core region are many; however, Savino and Ragsdale (35) presented some data from this region, using a disc-like vortex generator. A theoretical profile is shown on Figure 17, referenced to the experimental inlet conditions.

## 6.3 Viscid Flow Theory

The previous theoretical models represented the two limiting conditions for fluid flow, that of negligible fluid viscosity as described in Section 6.1 and that of infinite fluid viscosity as described in Section 6.2. In this section, the theory presented attempts to explain real fluid behaviour, since the actual fluid viscosity enters into the theoretical analysis. The general approach of the authors involved in the following analysis has been to solve the Navier-Stokes equations for axisymmetric rotating flow. Differences in the resulting solutions can be attributed to the imposition of different boundary conditions and to assumptions of the type of core phenomenon, and of fluid characteristics, such as compressibility.

6.3.1 Laminar Flow, Incompressible Theory

The first solution of the Navier-Stokes equations for a fluid vortex was done by Einstein and Li (12) who solved the equations for the tangential velocity distribution for the incompressible low-strength vortex. More recently, Deissler and Perlmutter (7), and Donaldson and Sullivan (13) have extended the first solutions by substitution of different boundary conditions, particularly in the core region.

The important assumptions as made by Einstein and Li are listed below.

1. The axis of rotation of the vortex corresponded to the Z-axis of a cylindrical co-ordinate system.
2. The flow was considered symmetric about the Z-axis.
3. Average velocities in the Z-direction were assumed negligible with respect to the tangential velocity.
4. Incompressible flow, two-dimensional for all radii greater than that of the exit hole radius, was assumed to exist in the vortex system.
5. The total flow exited in the Z-direction through a flow area defined by the exit hole radius concentric with the Z-axis, and passed out of the vortex system at one end boundary of the flow.
6. The other end boundary of the vortex system was defined by a free surface at ambient barometric pressure.

7. The flow in the core region was assumed to have a uniform velocity in the Z-direction.
8. At the radius of the exit hole, a change in the characteristic type of flow was considered to occur, from the ideal or inviscid type to the solid-body type flow. At this radius, the fluid shear stress and the tangential velocities were used to link the equations of the two flow regions.

Within the framework of these assumptions, the authors were able to solve the Navier-Stokes equations and calculate the dimensionless tangential velocity and angular momentum relations, referring them to their value at a reference radius which corresponded to the exit hole radius. The major independent variable in the equations was that of the radial flow Reynolds number, which incorporated the fluid viscosity and the radial mass flow per unit length of vortex. It was defined as;

$$\frac{\rho R}{\mu}\left(\frac{m}{\rho 2\pi R}\right)^{*} = \frac{m}{2\pi\mu} = A$$

In this expression, **A** is the Radial Reynolds number, as used in Einstein and Li's notation, m is the rate of radial mass flow through the vortex, and $\mu$ is the fluid viscosity. The equations for the dimensionless angular momentum are presented in the Appendix, Section 10.2.

Some preliminary results were obtained from the plexiglass vortex generator, and a tangential velocity distribution is

* "$\rho$" represents the fluid density

shown in Figure 16, for a Radial Reynolds number of 60., and an exit diameter of .50 inches. The velocities at a particular radial position were calculated using a photograph of the free surface of the vortex, and a numerical technique, as outlined in Einstein and Li's report, and described in the Appendix, Section 10.3. The preliminary results showed considerable scatter, and have been presented here only as indicative results, since considerable refinement of this method of measuring velocities would be required.

The theoretical predictions using Einstein and Li's theory, using a Radial Reynolds number of 60, and a reference radius of .25 inches was also shown on Figure 16, using the outermost experimental tangential velocity as a boundary condition. This prediction is essentially identical to the profile obtained using ideal flow theory, since the two theoretical models coincide when Radial Reynolds numbers of this magnitude are used in the relevant Einstein and Li relation.

### 6.3.2 Laminar Flow, Compressible Theory

When a theoretical analysis is applied to a gaseous vortex system, the assumption of incompressible fluids cannot be made, particularly when velocities approaching the speed of sound are considered. Pengelley (5) presented the solution of the Navier-Stokes equations for compressible flow. As

expected, the boundary conditions and assumptions for the incompressible case and the compressible case were reasonably similar, except for specific extensions related to fluid compressibility. Since the present study was concerned with high velocities, the compressibility effects would probably be significant, and as a result Pengelley's theory was reviewed in some detail. The assumptions in common with Einstein and Li's work were noted, while those assumptions which differ are presented below.

1. Assumptions 1,2,3, as made by Einstein and Li, listed under Section 6.3.1, were also made by Pengelley.
2. The flow was considered to be contained between two concentric rotating cylinders, the surface velocity of which established the tangential boundary conditions for the rotating flow.
3. The mass flow was assumed to pass radially through these concentric cylinders, their material necessarily being porus.
4. The fluid was considered to obey the perfect gas laws, and the entire system was assumed to be adiabatic, but non-isentropic.
5. The parameters of Pengelley's equations, the tangential velocities, temperatures, and pressures, were made dimensionless by referring them to their value at a reference radius. This radius was theoretically

defined as the position at which the change of angular velocity with radius was zero, and was physically interpreted as the point at which solid-body type flow existed.

Using these conditions Pengelley presented the tangential velocity, the temperature, and the pressure as a function of radius. The major variable in his equations was the Radial Reynolds number as in Einstein and Li's work.

The equation for the tangential velocity and its mathematical derivation is included in the Appendix, Section 10.4.

A typical experimental profile of the tangential velocity for the stainless-steel vortex generator is shown on Figure 17. The test was conducted with a 1.000 inch diameter exit, and a mass flow rate giving a Radial Reynolds number of the order of 2000. Theoretical profiles as predicted by Pengelley's theory are also shown on the same graph, using Radial Reynolds numbers of 2, and 3. It is obvious that the theoretical predictions are considerably different from the experimental values, even though the Radial Reynolds number had been decreased 1000 times before being used in the theory, in order to account for turbulent degradation of the vortex system.

As in Einstein and Li's theory, a Radial Reynolds number of the order of 100 or larger, when used in the theoretical equations, predicts a velocity profile which is essentially identical with that of the ideal or free vortex theory.

## 6.4 Semi-Empirical Analysis

As has been shown in earlier parts of this chapter, and also by other experimental comparisons, such as Donaldson(30), predictions of tangential velocities based on a wholly theoretical approach have been unable to closely compare with experimental results, particularly for vortex flows of reasonably large Radial Reynolds numbers. This prompted Holman and Moore (36) to produce a method of calculating tangential velocities which was partially dependent on experimentally evaluated constants for a particular vortex. Once these constants which were based on experimental static pressure measurements and inlet conditions, were evaluated, it would be possible to predict tangential velocities as a function of radius, sufficiently accurate for many engineering applications.

Their assumptions are listed below

1. A tangential velocity-radius relation of the following type was assumed to apply for the entire vortex

$$V_t R^n = \text{Constant}$$

The index n is the experimentally evaluated vortex exponent, and has a value of the order of 1.

2. A polytropic relation between pressure and temperature was assumed to apply throughout the vortex.

3. The solution of the Navier-Stokes equations, using assumption 1, showed that the stagnation temperature could be considered constant with radius for Radial Reynolds numbers of the order of 100 or larger. Since the vortex flows of their experiments used values of the order of 400 or more, they assumed a constant stagnation temperature.
4. Experimentally, it has been found that tangential velocities at the wall in a jet-driven vortex system are considerably lower than the inlet velocities from the jets. Holman and Moore, attempted to make possible the prediction of the wall vortex velocity by means of a parameter which was essentially a function of the inlet configuration. This parameter could be physically interpreted as an effective inlet area which was larger than the actual area, resulting in low predicted inlet velocities, when based on upstream conditions. The parameter was experimentally determined for a particular vortex configuration.

The index, n, was determined by plotting the experimentally determined static pressures for a particular vortex on logarithmic paper in such a way that the slope of this line became the value of n. A series of static pressures plotted in this way for several mass flow rates were experimentally

found by the authors to be parallel lines, for a particular vortex generator configuration.

Futhermore, once the index, n, was known it was possible to evaluate the inlet parameter, if the mass flow rate and properties of the working fluid upstream of the inlet were known, for one particular test condition.

A series of static pressures measured in this present study were plotted in the manner as described by Holman and Moore, and are shown in Figures 18 and 19. The vortex index, n*, was measured from the slopes, of the experimental curves, and used to predict tangential velocities. The profile obtained by this method was then plotted on Figure 17, in order to compare it with experimental velocity data, using as an inlet condition the outermost experimental data point. The inlet parameter was not calculated, since it was suspected that this part of the approach of Holman and Moore might not apply for a supersonic injection nozzle.

* "n" was found experimentally to have the value of approximately 0.7

# 7. DISCUSSION OF ERRORS IN THE EXPERIMENTAL WORK

## 1. Error Associated with Total Pressure Measurement

It was stated in the book Aerodynamic Measurements (38) that the assumption of isentropic compression at the tip of the probe was in error by less than $\pm$ .2% of the dynamic head for velocities up to Mach 1. The error due to misalignment of the probe with respect to the flow direction would be of the order $\pm$ .5% of the dynamic head for $10^{\circ}$ or less misalignment. This was based on work from the same reference. Viscous effects at the probe mouth could become significant if the Reynolds number at the mouth was below 30. In the present situation, using air and high velocities, the Reynolds number was of order 5000, and effects were insignificant. The geometric error in positioning the probe was approximately $\pm$ 0.010 inch.

| | |
|---|---|
| Assumption of isentropic compression at probe tip | $\pm$ .2% |
| Yaw angle | $\pm$ .5% |
| Probe error | $\pm$ .7% |

The probe error was $\pm$ .7% of the dynamic head. Considering a flow velocity of Mach .5 and air, the head would be of the order 10 In. Hg. Therefore, the probe error would be $\pm$ 0.007 X 10 = $\pm$ .07 In. Hg.

The error associated with measuring the probe stagnation pressure, when using mercury manometers consisted of two parts. The capillary error for a tube diameter of .25 inch is of the order ± .05 In. Hg. The reading error for the manometer scale was±.05 In. Hg. per reading. When reading both sides of a U-tube manometer, the possible error was ± .10 In. Hg.

| | |
|---|---|
| Order of capillary error | ± .05 In. Hg. |
| Reading error | ± .10 In. Hg. |
| Pressure measuring error | ± .15 In. Hg. |

The dial gauges were calibrated against mercury manometers, and as a result possessed a possible error of the same order.

The mercurial barometer was accurate to 1 part in 3000, as stated by the manufacturer.

| | |
|---|---|
| Probe error | ± .07 In. Hg. |
| Pressure measuring error | ± .15 In. Hg. |
| Total pressure error | ± .22 In. Hg. |

2. Error Associated with Static Pressure Measurement

A. Error inherent with Stagnation Probe turned through 90°

During the programme, attempts were made to measure the static pressure in the vortex system by turning the

stagnation probe (shown in Figure 5a) through 90° to the flow direction, and by adjusting it through a small angle to produce the minimum pressure. The pressures so measured were suspected of being in error, consequently a calibration was performed. The test apparatus consisted of a standard Prandtl pilot-static probe and a probe of similar geometry to that of Figure 5a, mounted near the end of a plexiglass tube of .75 inch I.D. Air was passed through this 5 foot long tube, and exhausted to the surroundings. At each flow rate, readings of the total and static pressures were made with each probe, and the difference in the measured quantities calculated. The Mach number was obtained using readings of the Prandtl probe. Some indicative results are included in the following table.

| | | | | |
|---|---|---|---|---|
| Mach number | .28 | .34 | .41 | .48 |
| Static pressure difference (In. Hg.) | 1.40 | 2.30 | 3.90 | 5.00 |
| Total pressure difference (In. Hg.) | .05 | .18 | .20 | .35 |

These results showed that pressures obtained by turning a stagnation probe through 90° were not the static pressures but were in fact, some pressure less than the static in all cases. Consequently, this measuring technique was not used to calculate the Mach numbers shown in Figures 10 and 11. A graphic example of the discrepancy in Mach number resulting from using both methods of measuring the static pressure

is shown in Figure 22.

B. Error inherent with End Wall Static Pressure Measurement

When using a static hole of small diameter (.020 In. diameter) the error was quite small. Aerodynamic Measurements data was presented showing the error to be approximately .2% of the dynamic head. Considering a dynamic head of 10 In. Hg. this error would be $\pm$ .002 X 10 = $\pm$ .02 In. Hg. The pressure measuring error would be the same as in part A, approximately $\pm$ .15 In. Hg.

| | |
|---|---|
| Hole error | $\pm$ .02 In. Hg. |
| Pressure measuring error | $\pm$ .15 In. Hg. |
| Static pressure error | $\pm$ .17 In. Hg. |

The total calculated error associated with the end wall static pressures was of the order $\pm$ .17 In. Hg. This small error would tend to give a false indication of the accuracy of measurement, since the flow phenomenon at the end plate was quite complex, and not understood. As a result, no conclusion could be drawn as to the actual error associated with the static pressures measurement in this region, but it was thought to be larger than the calculated error, due to the three-dimensional effects.

3. Error Associated with Temperature Measurement.

A. Error involved in Total Temperature Measurement in Upstream Air.

The error involved in this measurement was largely due to the uncertainty for an uncalibrated thermocouple. In the range of temperatures 75° F. to 200° F., the manufacturer's tolerance was ± 1½° F. The temperature of the ice bath was considered to be 32.0 ± .2° F. Millivolt potential could be measured to approximately ± .002 millivolt, corresponding to .1° F. The thermocouple was located in a region with a large flow area, resulting in low velocities, consequently, the temperature of the thermocouple could be assumed to be that of the total temperature of the air.

| | |
|---|---|
| Two copper-constantan thermocouple junctions with manufacturer's guaranteed tolerance of ± 1½° F. per junction. | ± 3.° F. |
| Ice-bath reference temperature (distilled water). | ± .2° F. |
| Potentiameter error (when properly adjusted). | ± .1° F. |
| Total error possible | ± 3.3° F. |

B. Error involved in Temperature Measurement through the Vortex.

Since a thermocouple exposed to a high velocity air

stream reaches some temperature which is less than the fluid total temperature, the relation between these temperatures offered the most uncertainty in this measurement. The manufacturer's guarantee for the iron-constantan 30 gauge, Brown and Sharpe, uncalibrated thermocouple was $\pm$ 4° F. for the range of temperatures from 0° F. to 530° F. Assuming a distilled water ice-bath, the temperature of the reference junction was considered to be 32.0 $\pm$ .2° F.

| | |
|---|---|
| Two iron-constantan thermocouple junctions with manufacturer's guaranteed tolerance of $\pm$ 4° F. per junction | $\pm$ 8.° F. |
| Ice-bath reference temperature (distilled water) | $\pm$ .2° F. |
| Potentiometer error (when properly adjusted) | $\pm$ .15° F. |
| Total error possible | $\pm$ 8.35° F. |

This represented the possible error associated with the actual temperature of the thermocouple junction. In order to evaluate the temperature of the vortex flow around the junction, it was necessary to use the results of other experimental investigations for recovery factors for butt-welded thermocouples. One such investigation was that of Simmons (37). He related the two temperatures mainly as a function of Mach number, and presented data which permitted the evaluation of the total temperature from the thermocouple temperature to an accuracy of $\pm$.5%, based on the

absolute temperature. Specifically, he showed that the thermocouple temperature was 98% to 99.5% of the total temperature for a Mach number range between .25 and .50, based on the absolute temperatures.

The possible error associated with the total temperature evaluation, when considering a thermocouple temperature of 530° R (see Figure 12) is shown below

| | |
|---|---|
| Error involved in thermocouple temperature | ± 8.35° F. |
| Error involved using Simmons (37) recovery ratios (½% of 530° R) | ± 2.7° F. |
| Total error possible | ±11.2° F. |

Considering the magnitude of this error, it was concluded that the error involved in assuming the thermocouple temperature equal to the total temperature would not be significant, since the maximum correction at Mach .5 would be 2% X 530 = 10.6° F. It was therefore valid to consider the profiles of Figure 12 representative of the total temperatures in the vortex, with an uncertainty of approximately 11° F.

## 8. Conclusions

Tangential Mach numbers based on experimentally measured static and total pressures are presented for the stainless steel vortex generator, using 1.000 and 2.000 inch exit hole diameters for a range of upstream pressures. The maximum value measured was of the order Mach .7, this being obtained using the 2.000 exit diameter end plates. One value obtained by the above method was compared to results of a direct velocity measurement using a paddle-wheel in the flow, and the values were found to differ by 20%.

On the basis of experimentally determined effective temperature profiles taken radially through the vortex using a bare butt-welded thermocouple, the assumption of constant total temperatures appeared to be well-founded.

The flow in vortex generator was concluded to be reasonably two-dimensional, particularly in the annular regions. The experimental evidence supporting this conclusion was based on vortex cylinder wall static pressure measurements, on total pressure data at different axial locations, and on direct velocity measurement data using a paddle-wheel in the flow. Symmetry about the axis of rotation of the flow was also present, and coincidence of this axis of rotation with that of the geometric axis of the vortex chamber appeared to exist. The experimental evidence verifying this conclusion was based on results of radial static pressure surveys at different angular positions.

Probe interference effects in the vortex flow were generally present in all cases, although some probe designs and traversing positions caused much less disturbance than others. The apparatus used for the majority of the test results, was thought to give the least interaction of all the designs, this conclusion being reached after investigating two probin positions and eight different probe designs.

Analytical comparisons were described in Section 6, and the general conclusion made that theoretical predictions based on laminar flow assumptions does not well predict either the absolute value or the trend of the tangential velocities. Futhermore, the theoretical work was unable to analyze the complex phenomenon occurring during the injection phase of jet-driven vortex flows. The semi-empirical analysis as described in Section 6.4 appeared to describe the vortex flows better than other methods at the present time, and was in fact, the only available means of describing the inlet region of the vortex flow. However, experimental verification would be required to show the generality of the technique for inlet nozzles of all types, including the convergent-divergent nozzle acting under choked conditions.

A bi-stable vortex state was observed at some combinations of exit hole diameters and pressure ratios, this being obvious because of the change in noise level and fluctuation of wall pressures. It was thought to be associated

with the transition between one-celled and two-celled vortex structures, and in fact due to the oscillation from one type of vortex structure to the other. The exit hole velocity distribution for the two-celled type of vortex is shown in the illustrations, for one particular set of test conditions, and the large mass of air inducted from outside the vortex chamber should be noted. Occasionally, with certain combinations of outlet diameters and of upstream pressures, the central core region of the vortex would become sufficiently cold to condense the water vapor, and a white rotating cloud resulted. This condition was never observed with a one-celled vortex type, although a conclusion relating the two phenomenon cannot be made because of insufficient experimental evidence.

Noise levels of the order 140 decibels were experimentally measured, and preliminary tests showed the noise to be a function of the exit hole geometry since the imposition of a tube on the outside of the end disc of the same diameter as the exit hole, or the insertion of a porous tube in the core region both reduced the noise level considerably.

# 9. ILLUSTRATIONS

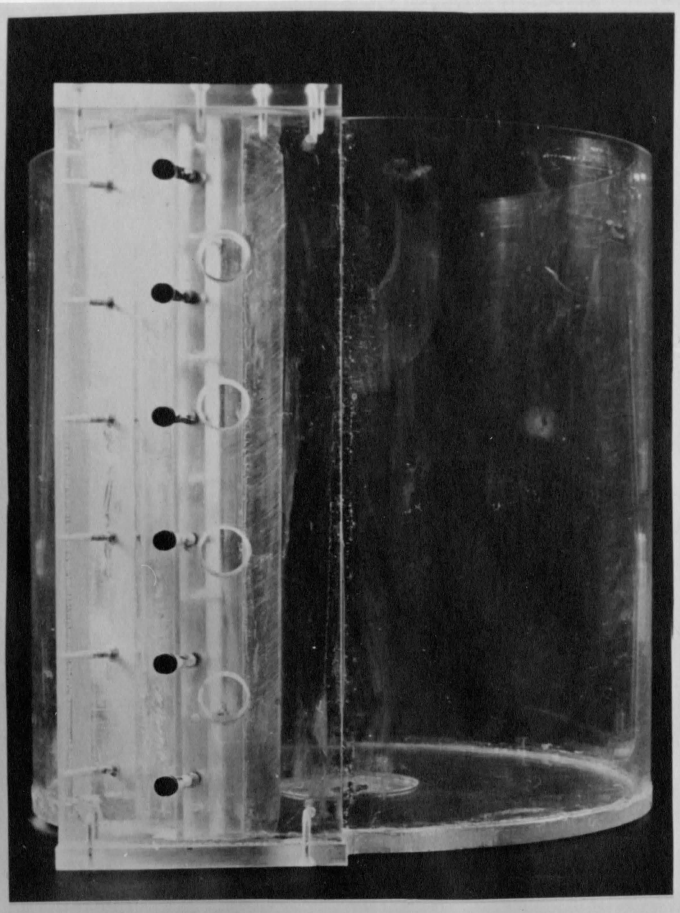

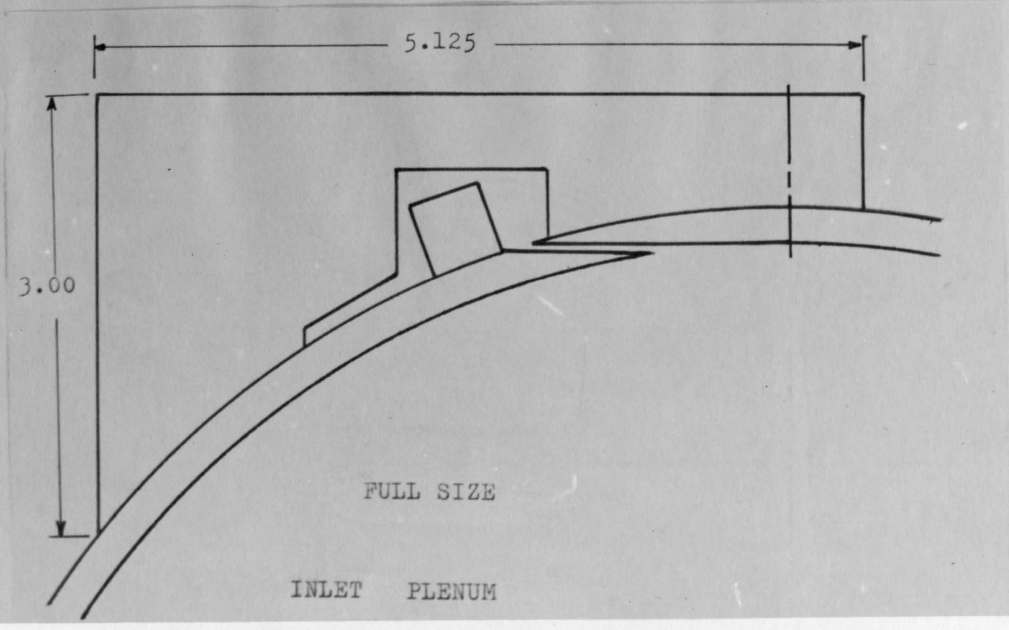


Fig. 1-Plexiglass Vortex Generator

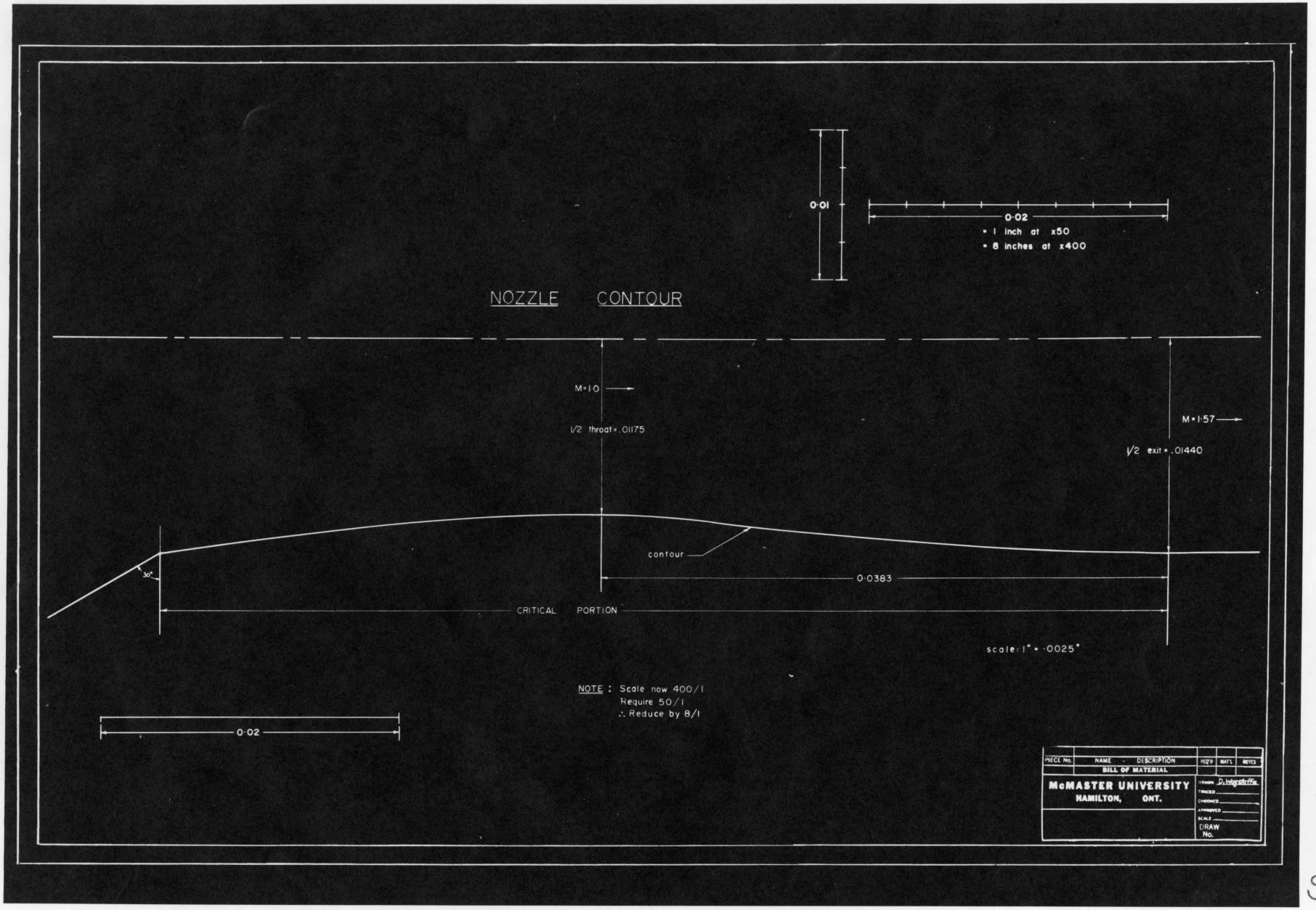
0·01
0·02
= 1 inch at x50
= 8 inches at x400
NOZZLE CONTOUR
M=1·0
1/2 throat = .01175
M=1·57
1/2 exit = .01440
contour
30°
0·0383
CRITICAL PORTION
scale: 1" = ·0025"
NOTE : Scale now 400/1
Require 50/1
∴ Reduce by 8/1
0·02
PIECE No.
NAME - DESCRIPTION
REQ'D
MAT'L
NOTES
BILL OF MATERIAL
McMASTER UNIVERSITY
HAMILTON, ONT.
DRAWN
TRACED
CHECKED
APPROVED
SCALE
DRAW No.

Fig. 2

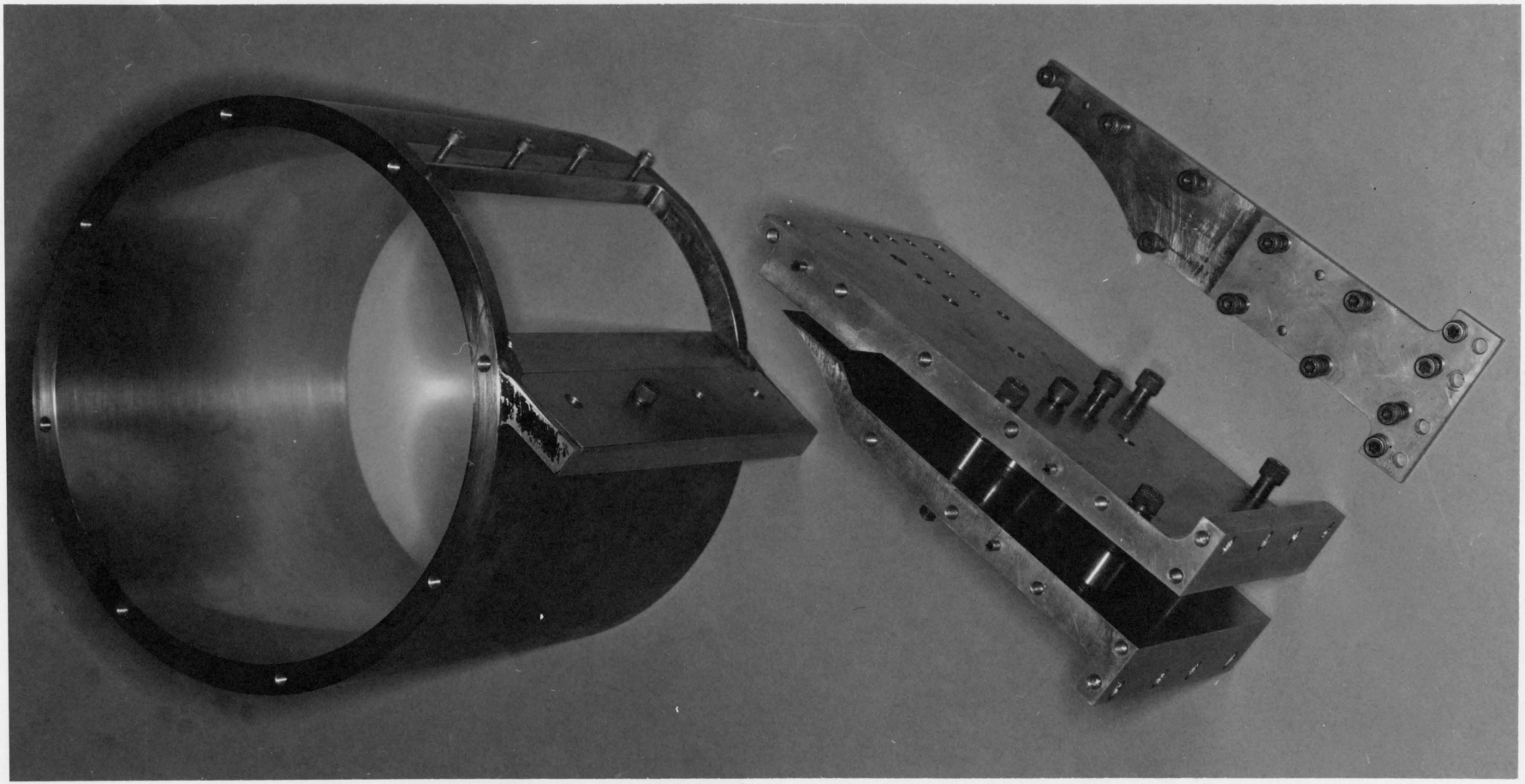

Fig. 3-Stainless Steel Vortex Generator and Nozzle

Fig. 4-End Plates

Steel End Plate

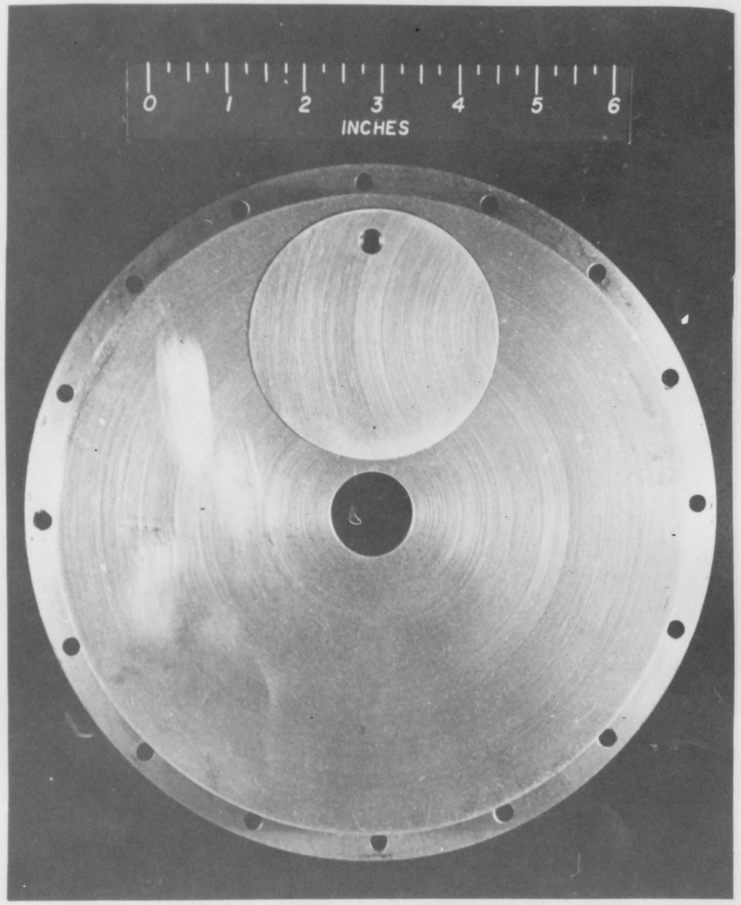


Plexiglass End Plate

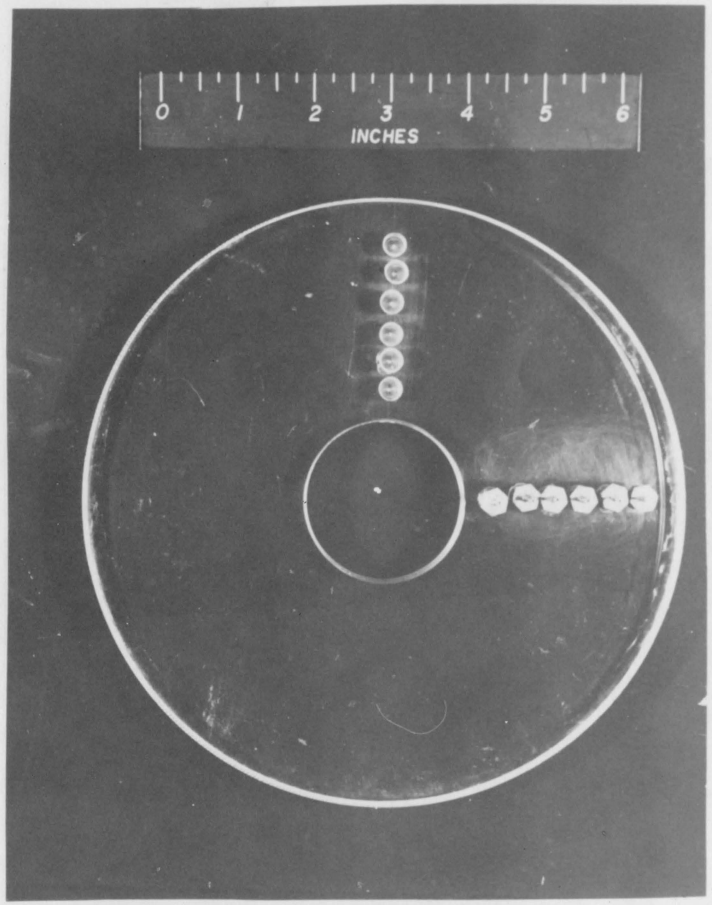

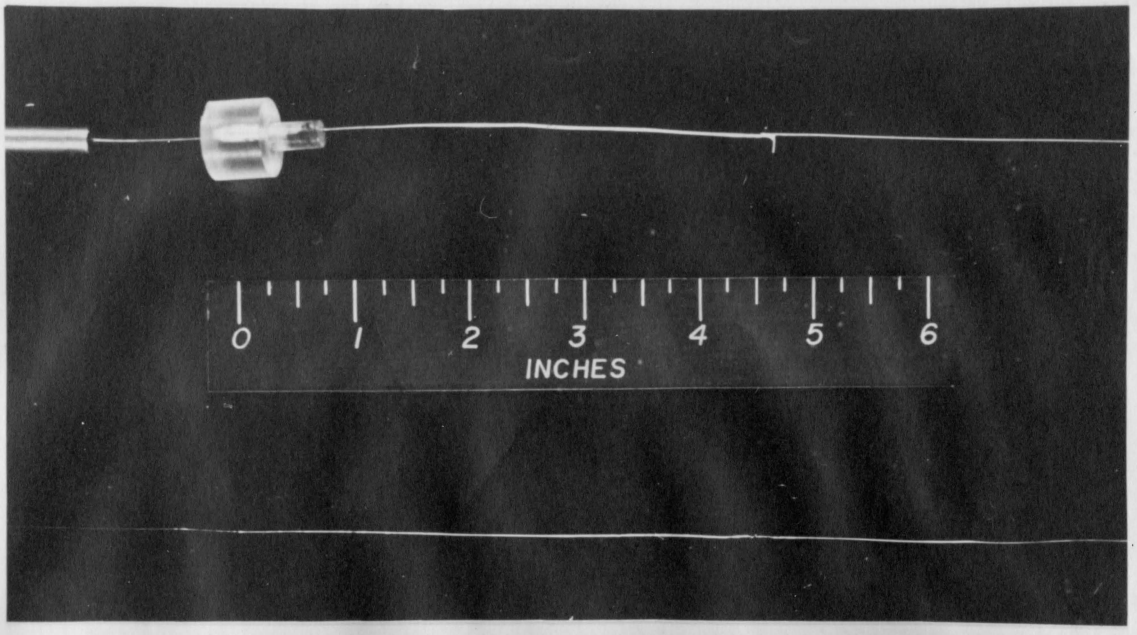


A

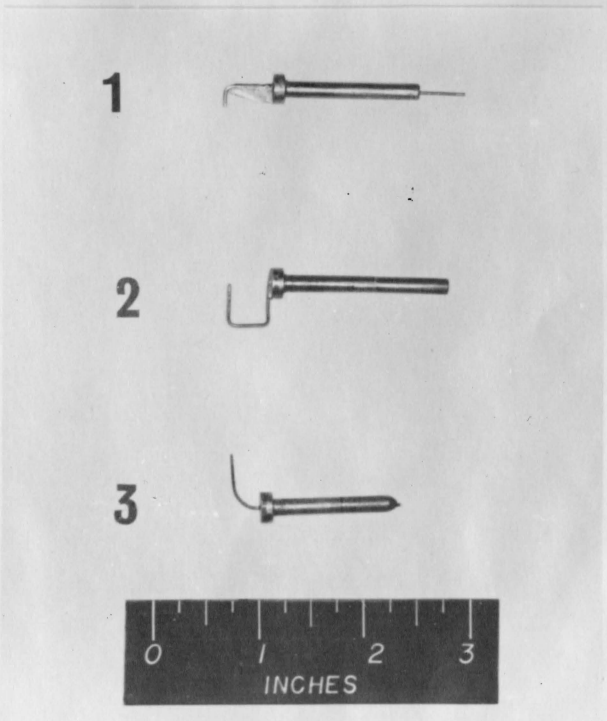


B

Fig. 5-Pressure and Temperature Probes

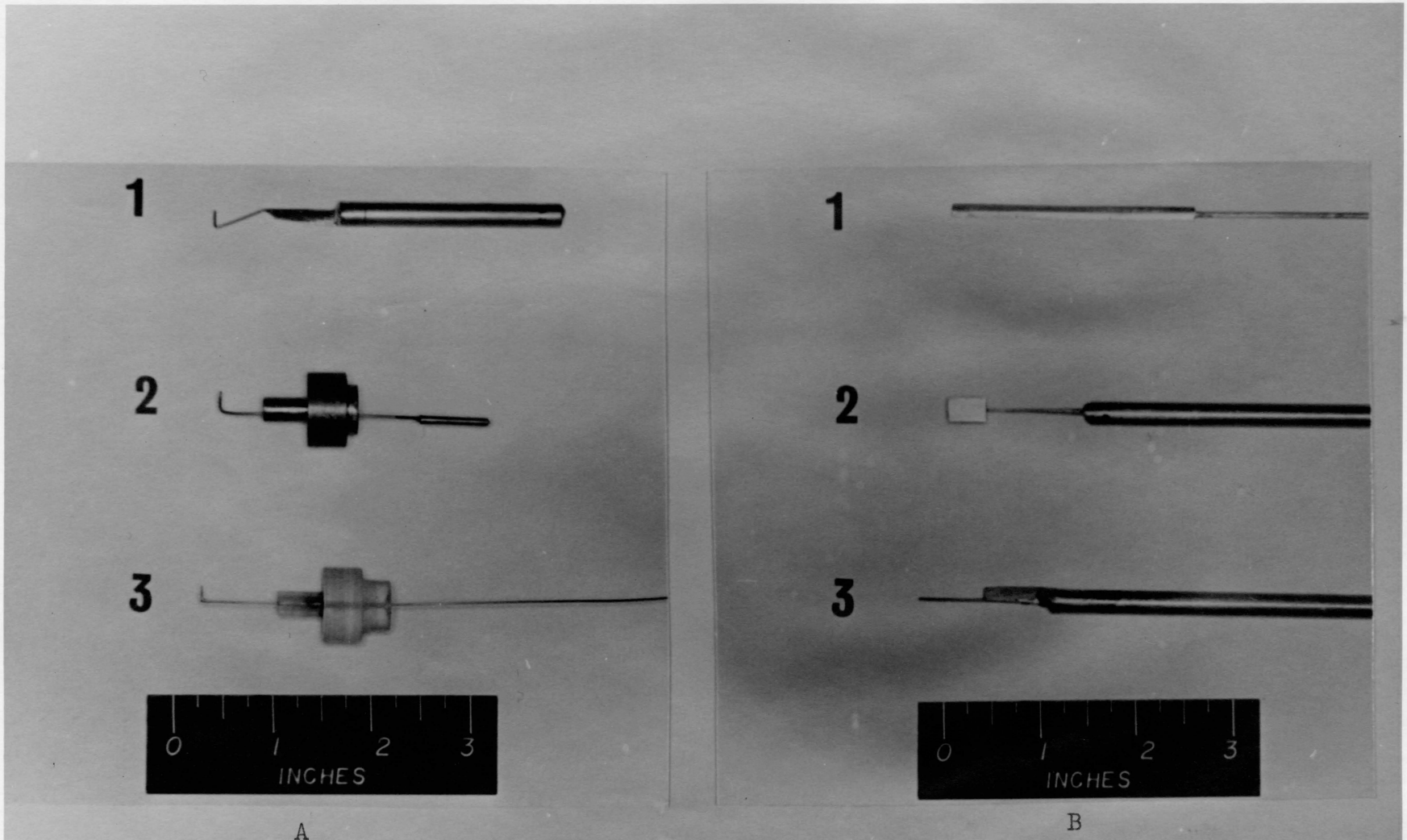


Fig. 6-Total and Static Pressure Probes

Fig. 7-Paddle-Wheel Velocity Measuring Apparatus

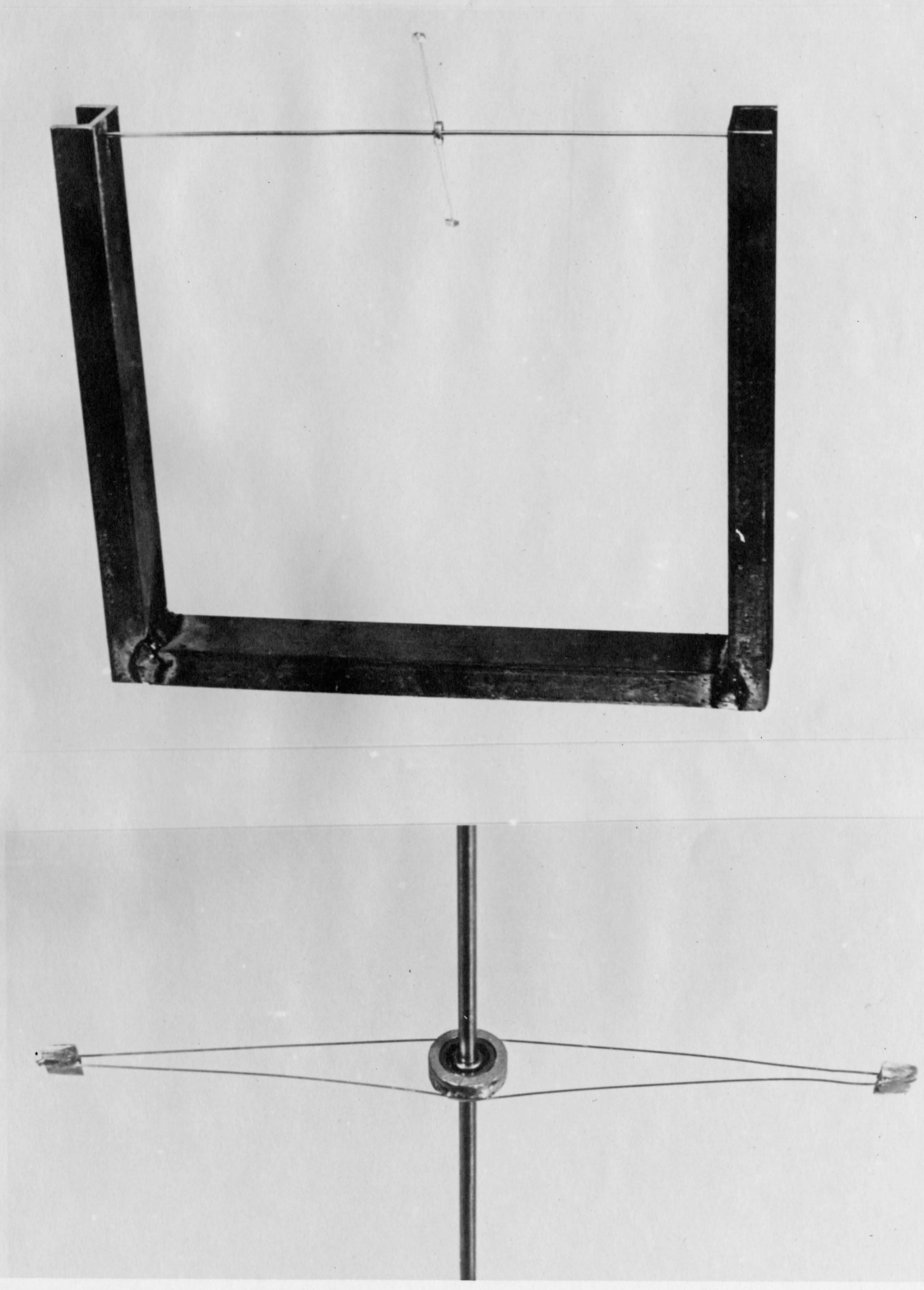

Fig. 8-End Wall Static Pressure

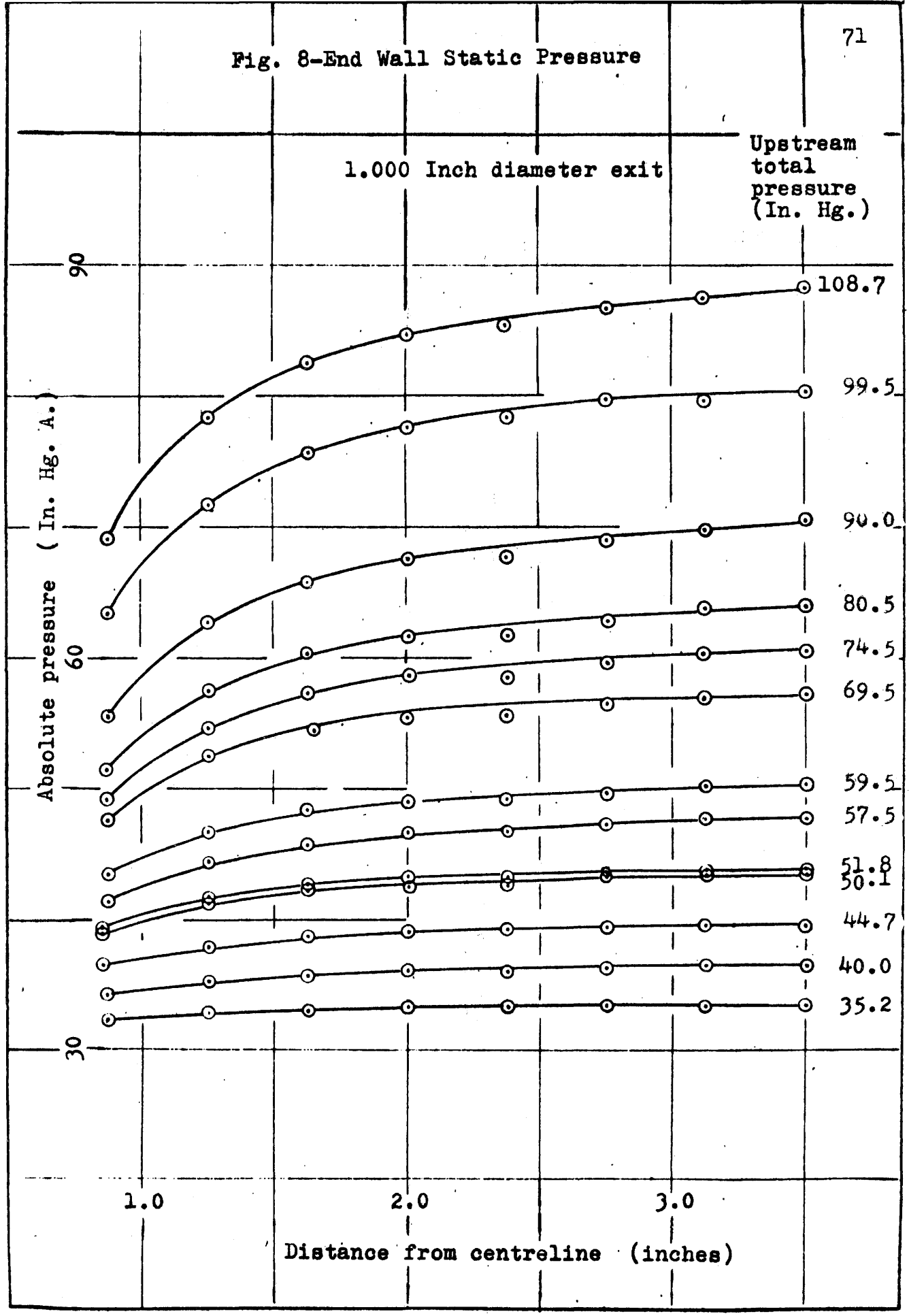

Fig. 9-End Wall Static Pressure

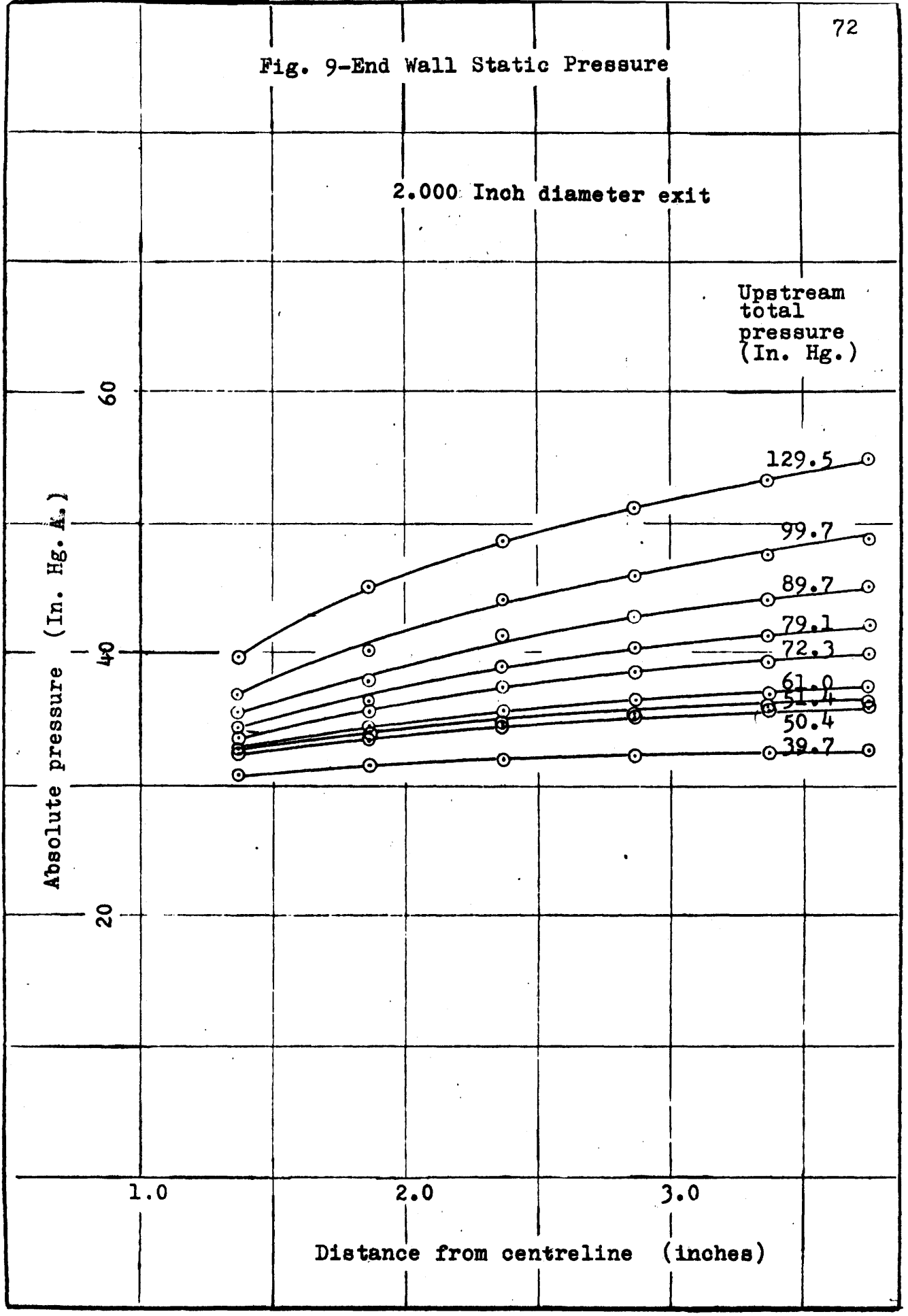

Fig. 10-Tangential Mach number Distribution

2.000 Inch diameter exit

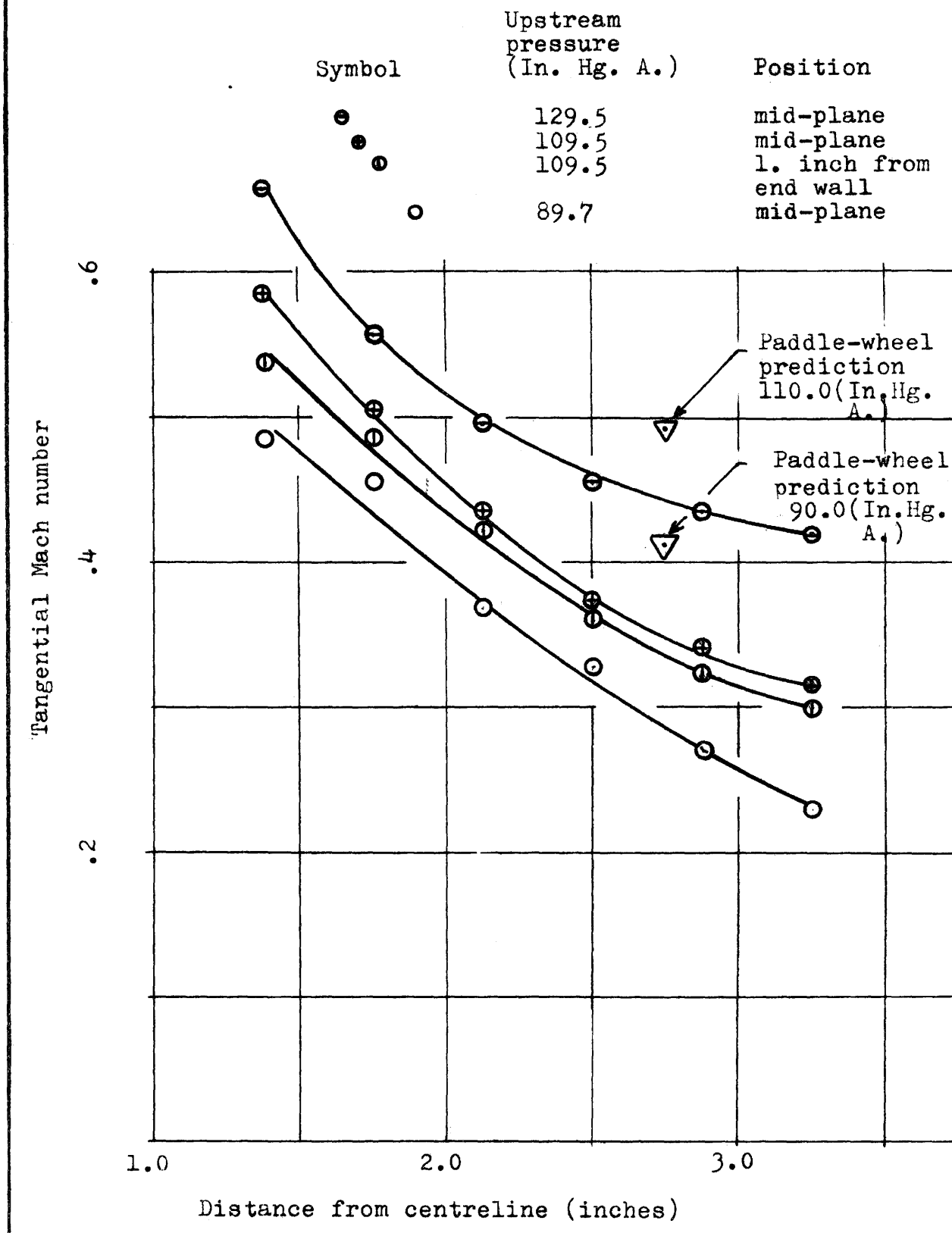

Fig. 11-Tangential Mach number Distribution

1.000 Inch diameter exit

| Symbol | Upstream pressure (In. Hg. A.) | Position |
|---|---|---|
| ⊖ | 80.7 | mid-plane |
| ⊕ | 59.6 | mid-plane |
| ⊖ | 49.5 | mid-plane |

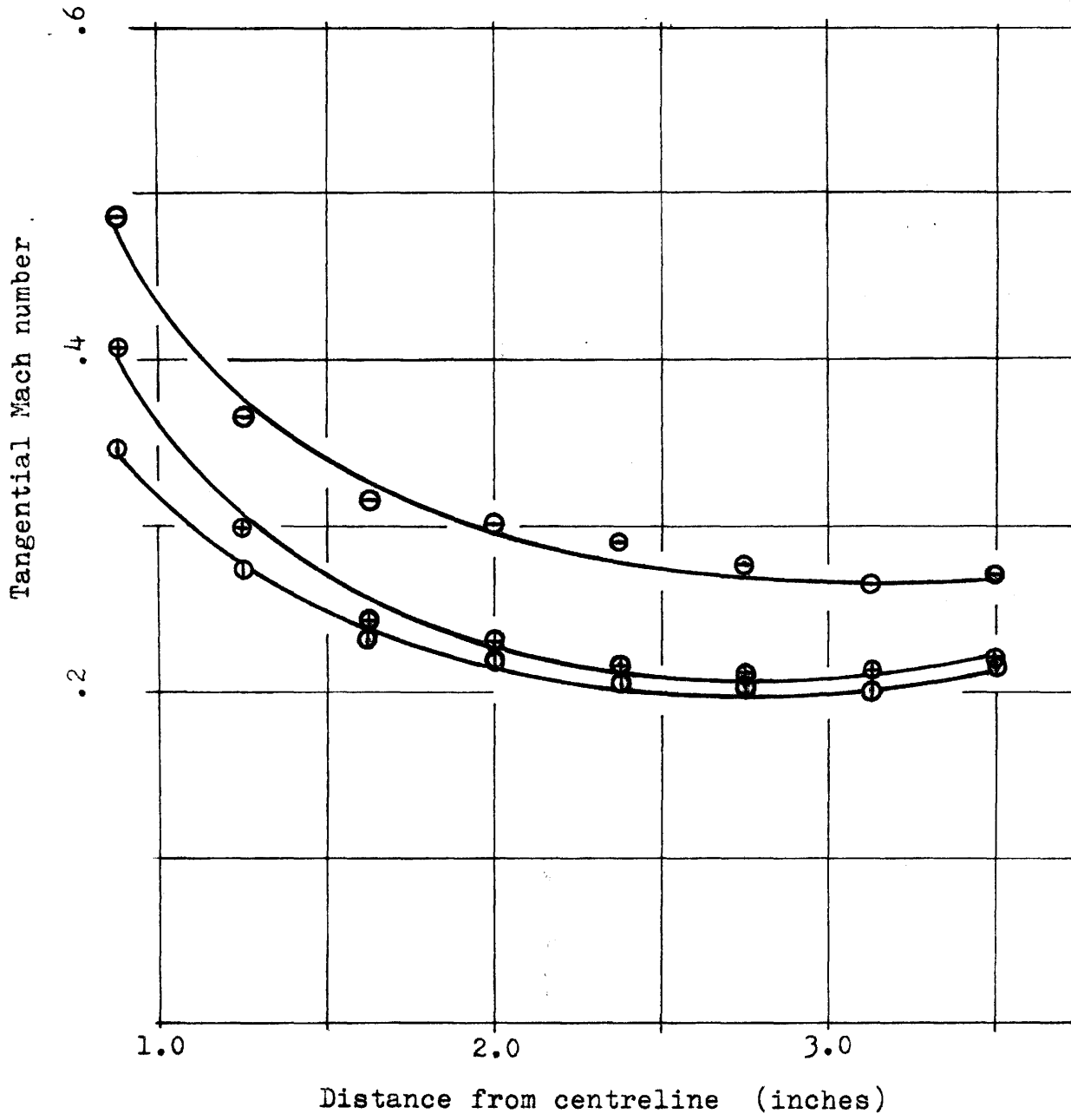

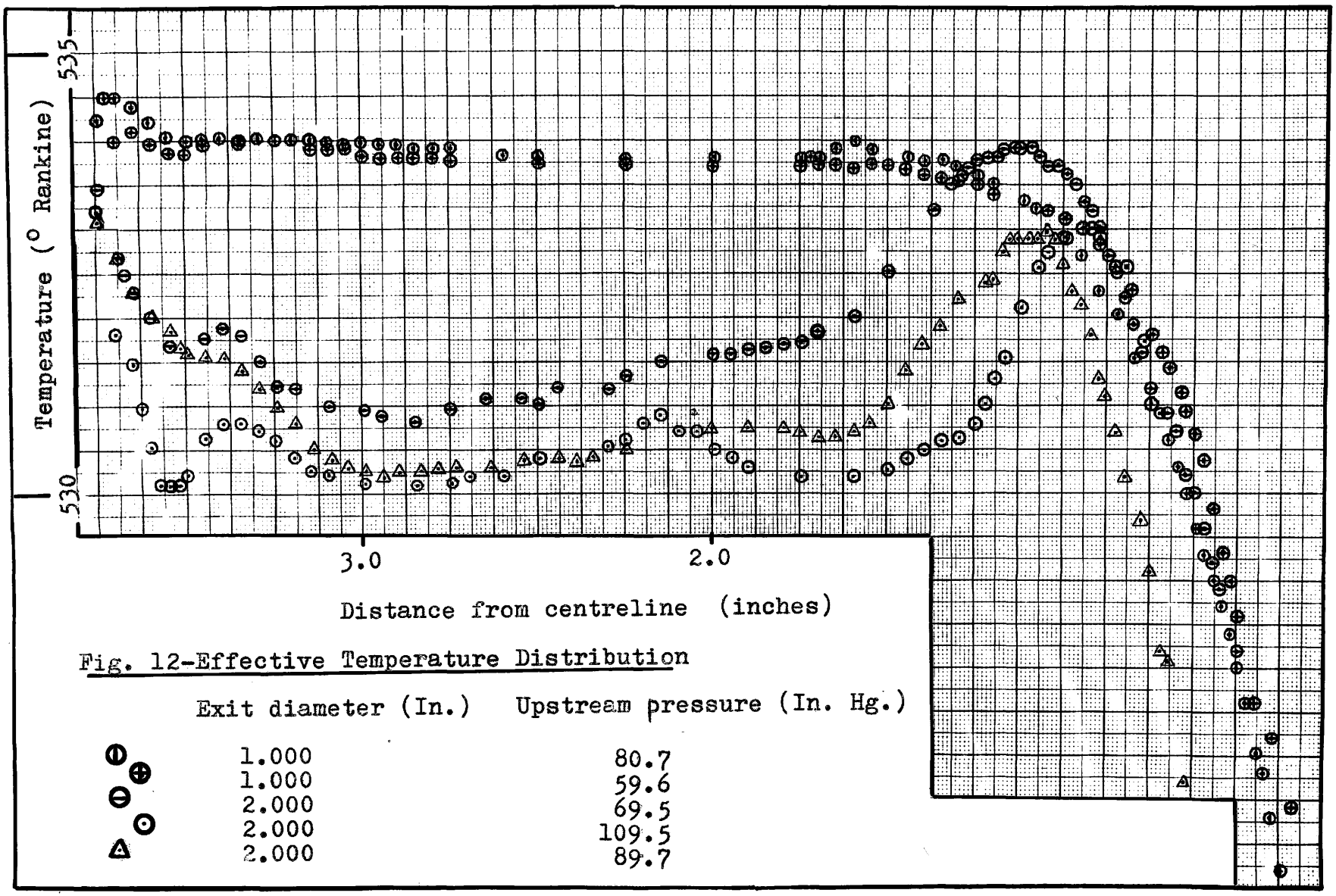


Fig. 12-Effective Temperature Distribution

| | Exit diameter (In.) | Upstream pressure (In. Hg.) |
|---|---|---|
| ⊕ | 1.000 | 80.7 |
| ⊖ | 1.000 | 59.6 |
| ⊙ | 2.000 | 69.5 |
| △ | 2.000 | 109.5 |
| | 2.000 | 89.7 |

Fig. 13-Results of Direct Measurement of Velocity

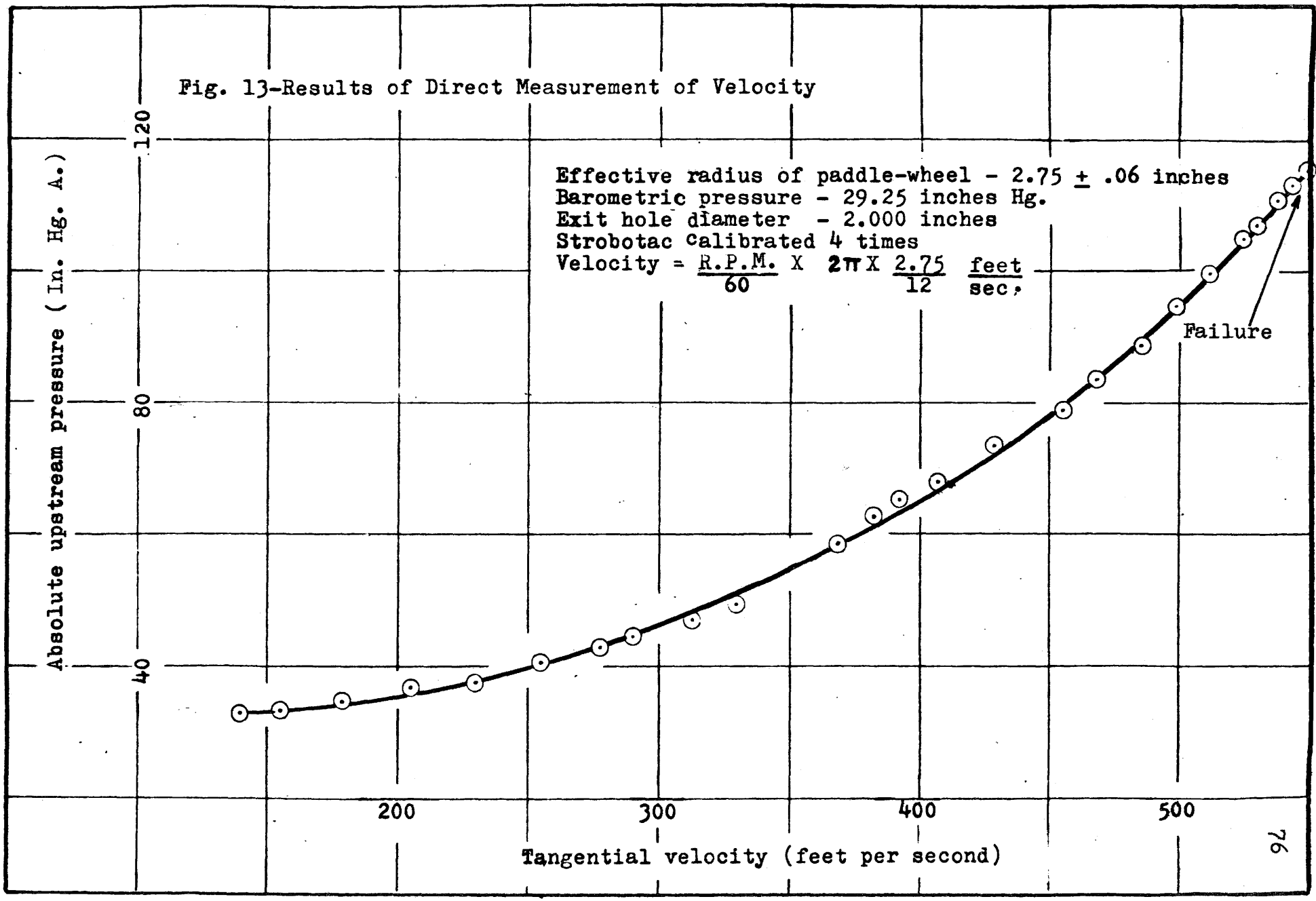

Fig. 14-Exit Hole Velocity Map

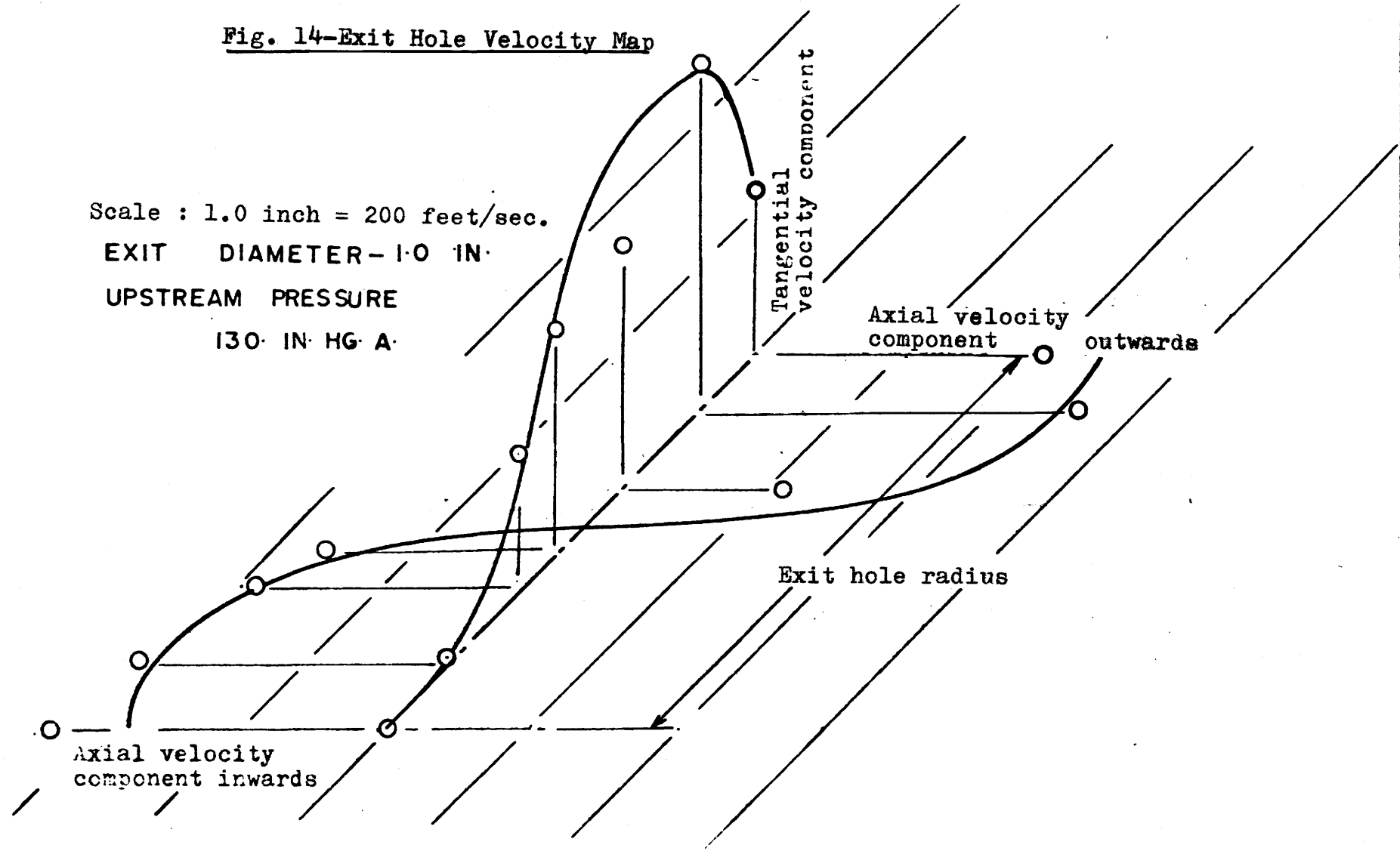

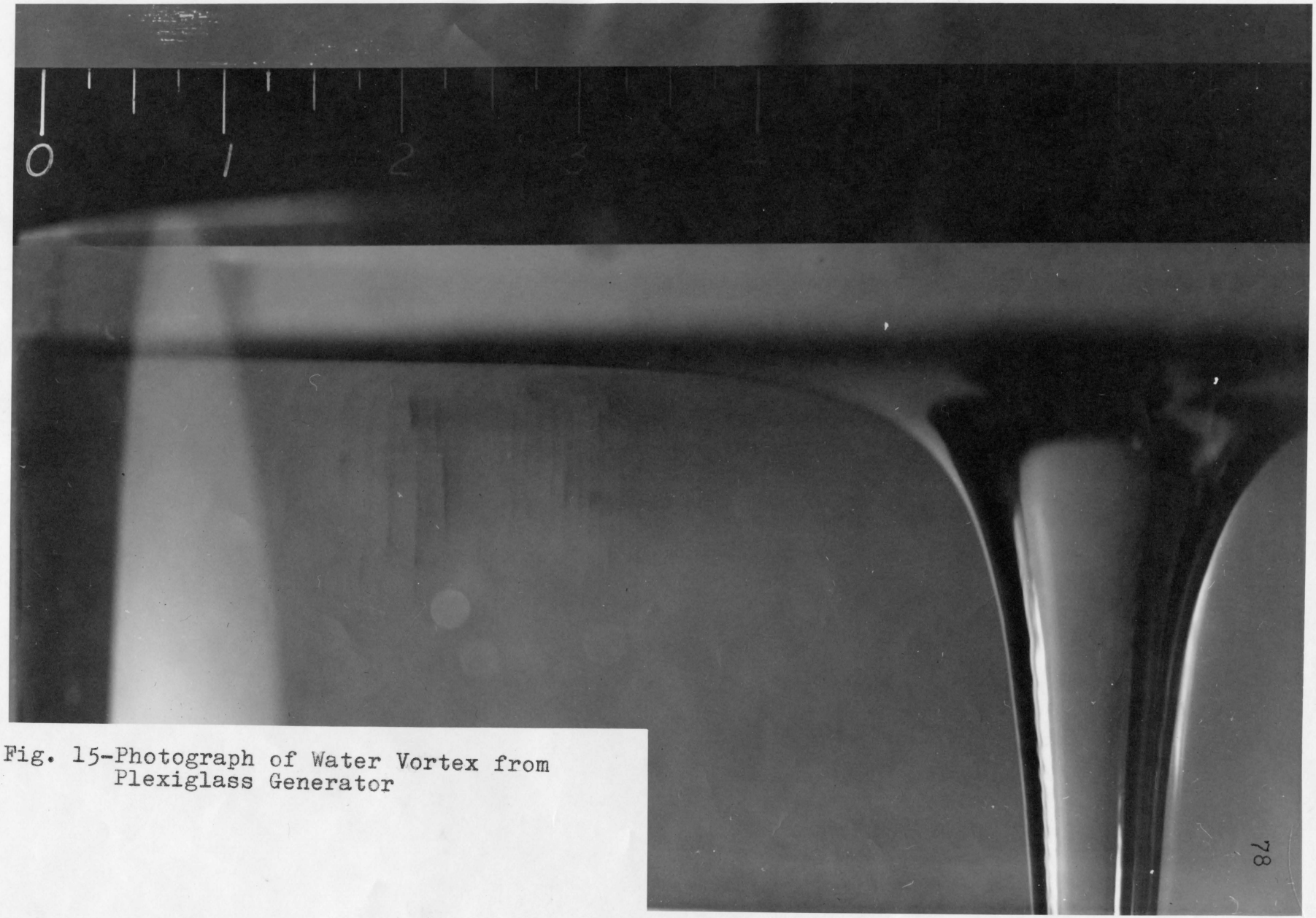


Fig. 15-Photograph of Water Vortex from Plexiglass Generator

Fig. 16-Experimental Tangential Velocities - Water Vortex

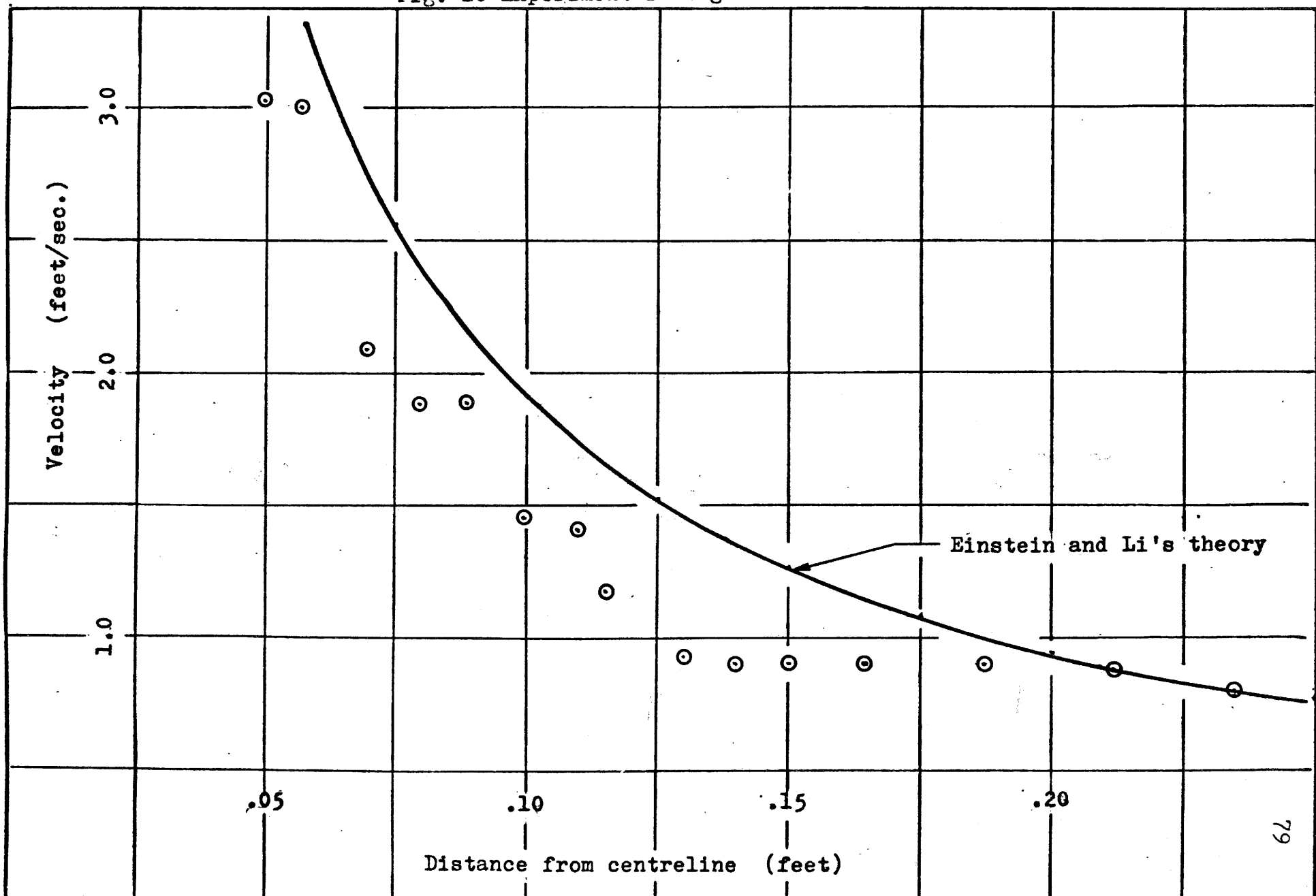

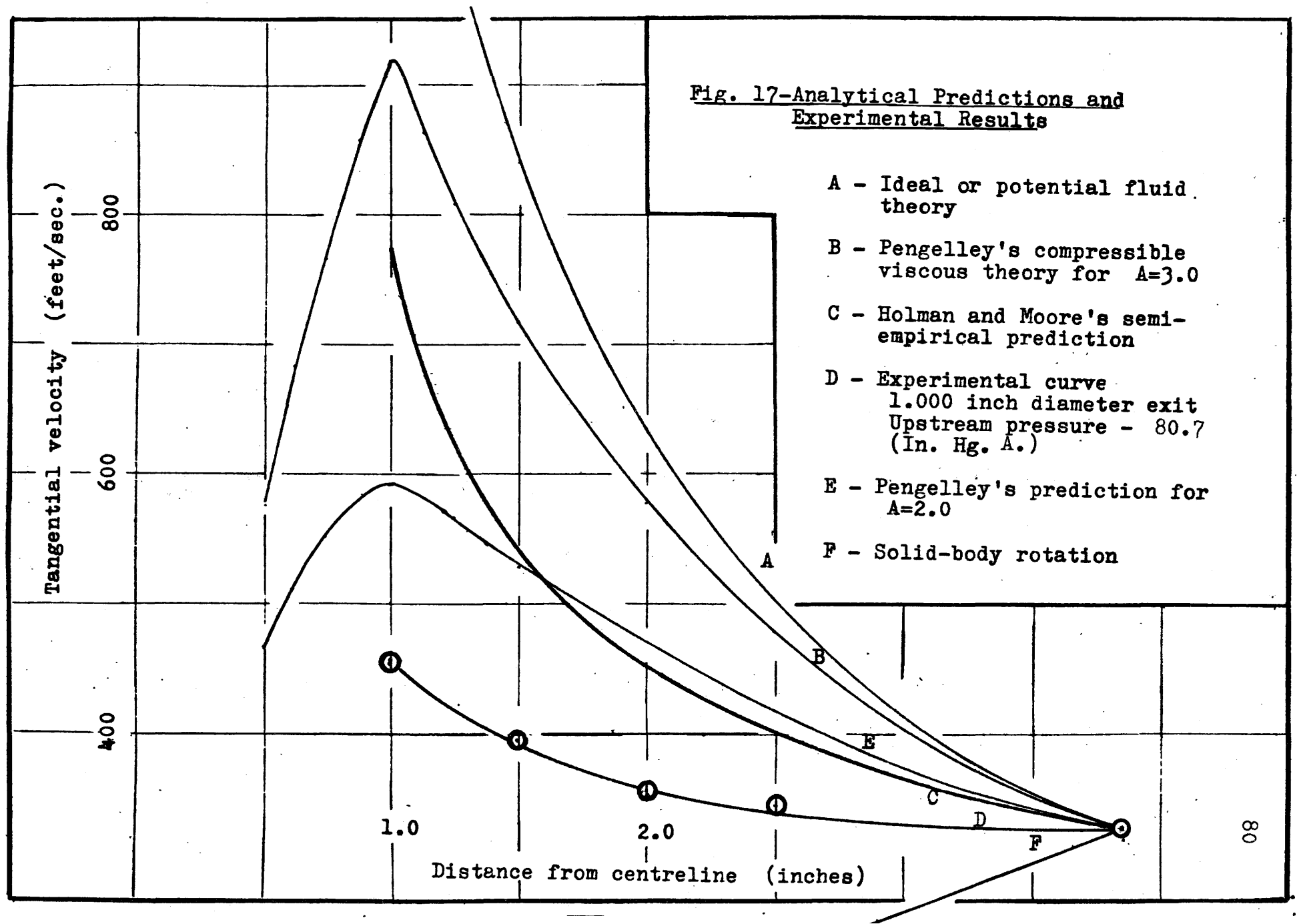
Fig. 17-Analytical Predictions and Experimental Results
A - Ideal or potential fluid theory
B - Pengelley's compressible viscous theory for A=3.0
C - Holman and Moore's semi-empirical prediction
D - Experimental curve 1.000 inch diameter exit Upstream pressure - 80.7 (In. Hg. A.)
E - Pengelley's prediction for A=2.0
F - Solid-body rotation
Tangential velocity (feet/sec.)
800
600
400
1.0
2.0
Distance from centreline (inches)
A
B
C
D
E
F
80

Fig. 18-Static Pressure Plotted to show Isentropic Deviation
1.000 Inch diameter exit

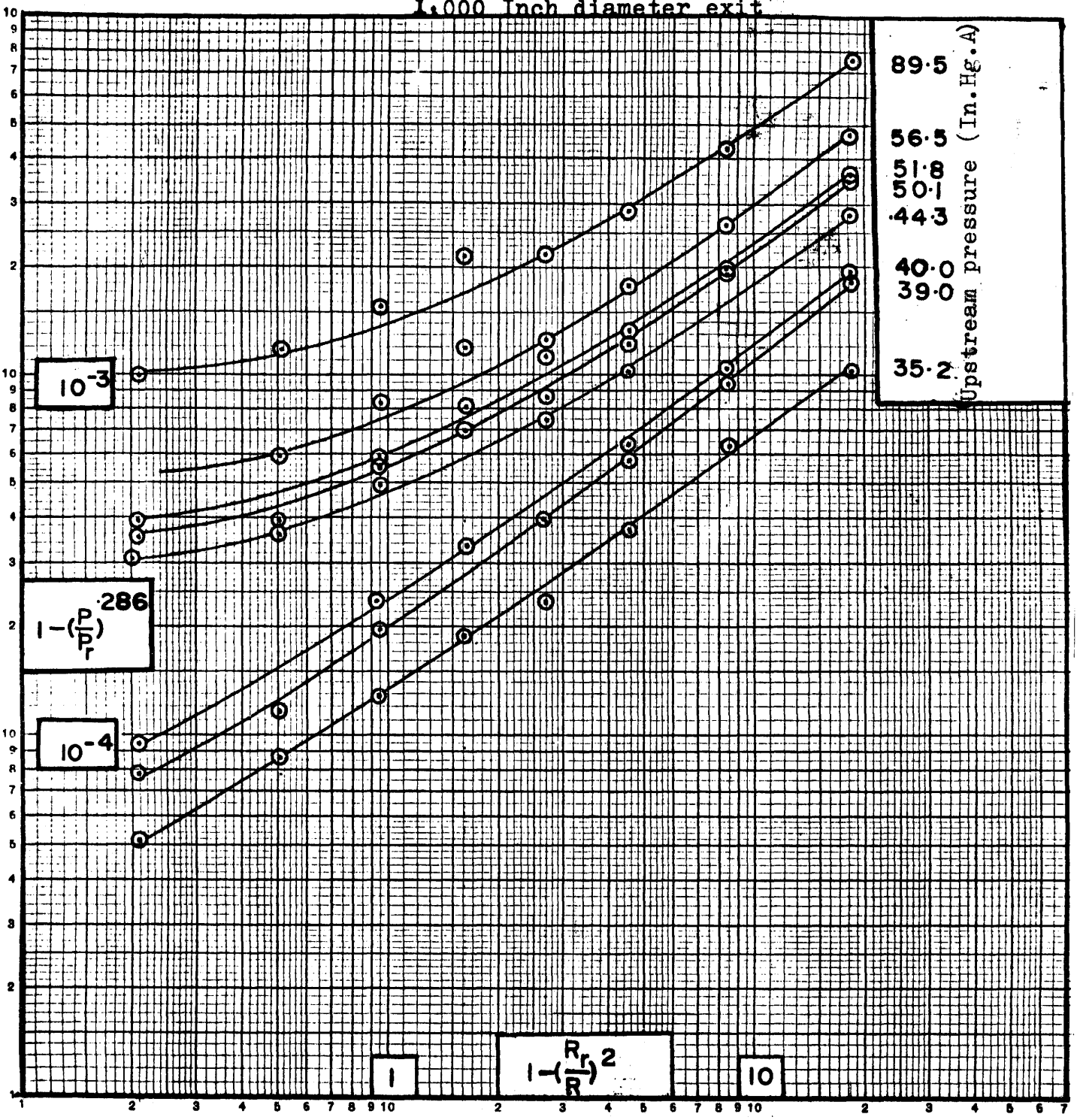


**P = $P_r$ and R = $R_r$ at the outer wall**

An average value of the vortex exponent "n" was found to be 0.7

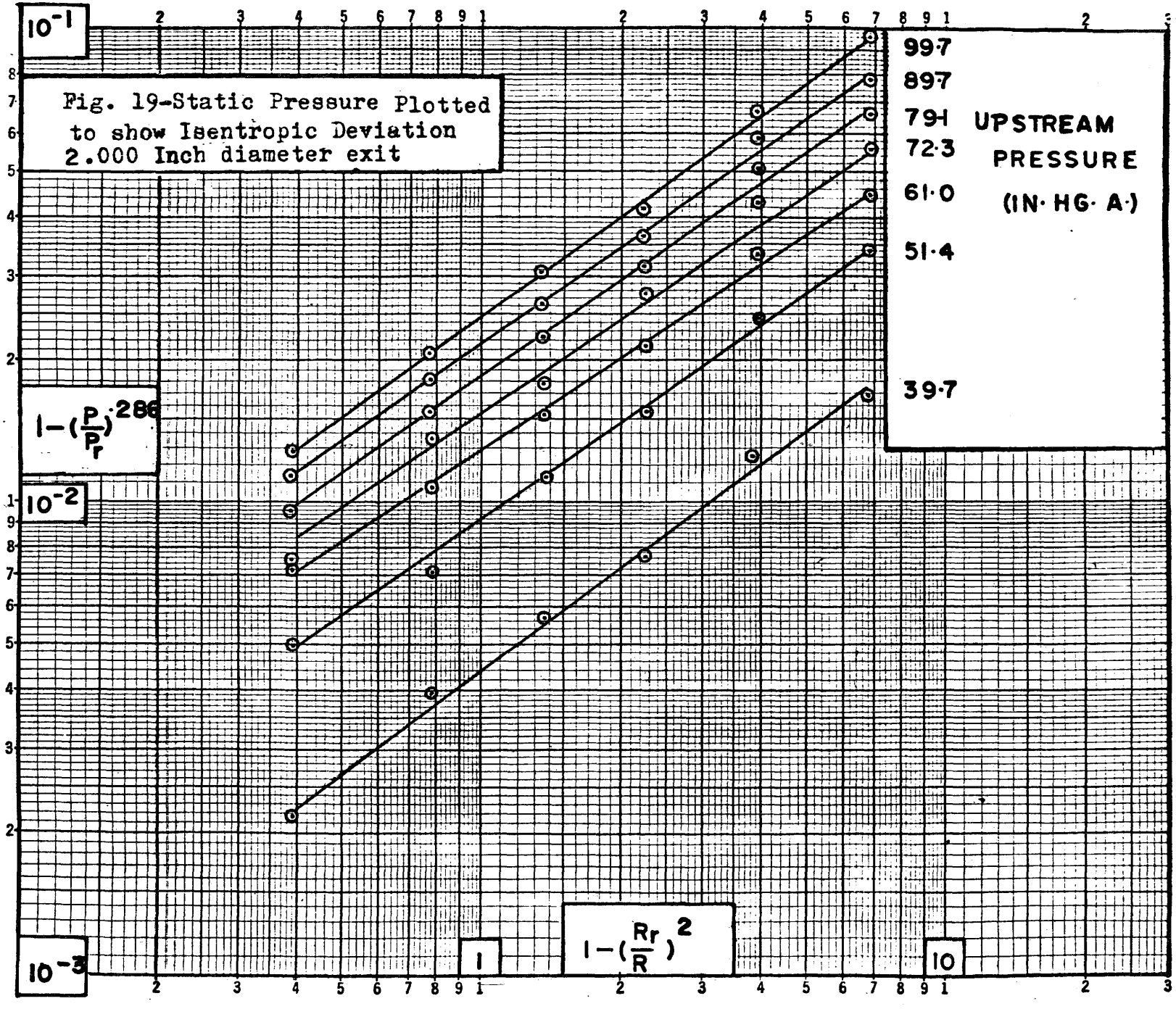
Fig. 19-Static Pressure Plotted to show Isentropic Deviation 2.000 Inch diameter exit
99.7
89.7
79.1
72.3
61.0
51.4
39.7
UPSTREAM PRESSURE (IN. HG. A.)
$1-(\frac{P}{P_r})^{.286}$
$1-(\frac{R_r}{R})^2$
$10^{-1}$
$10^{-2}$
$10^{-3}$
1
10

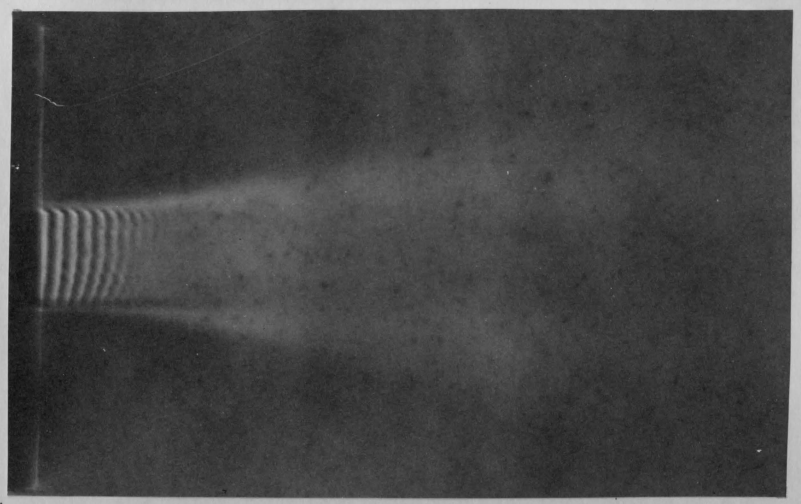

Flow from inlet nozzle (viewed along length of nozzle when tilted 15°)

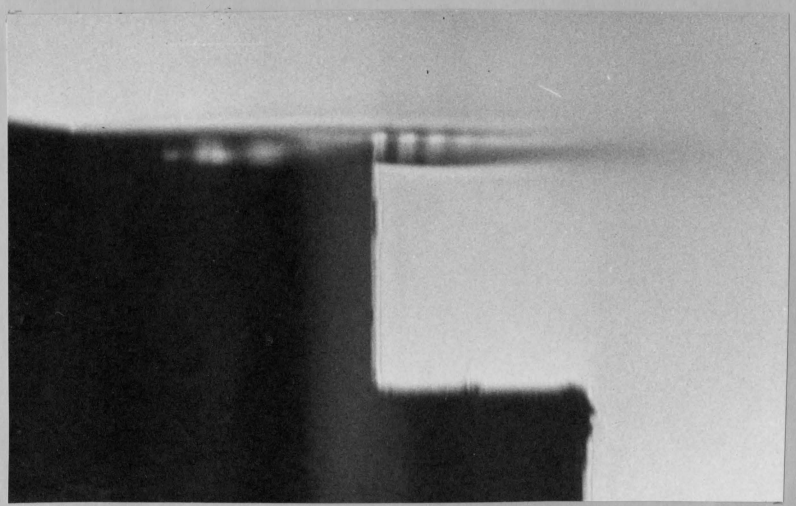

Flow from inlet nozzle (removed from cylinder)

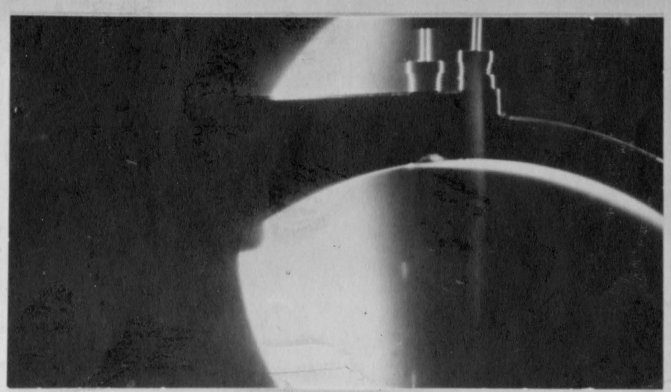

Region of flow impingement on cylinder wall

Fig. 20-Schlieren Patterns at Inlet Nozzle

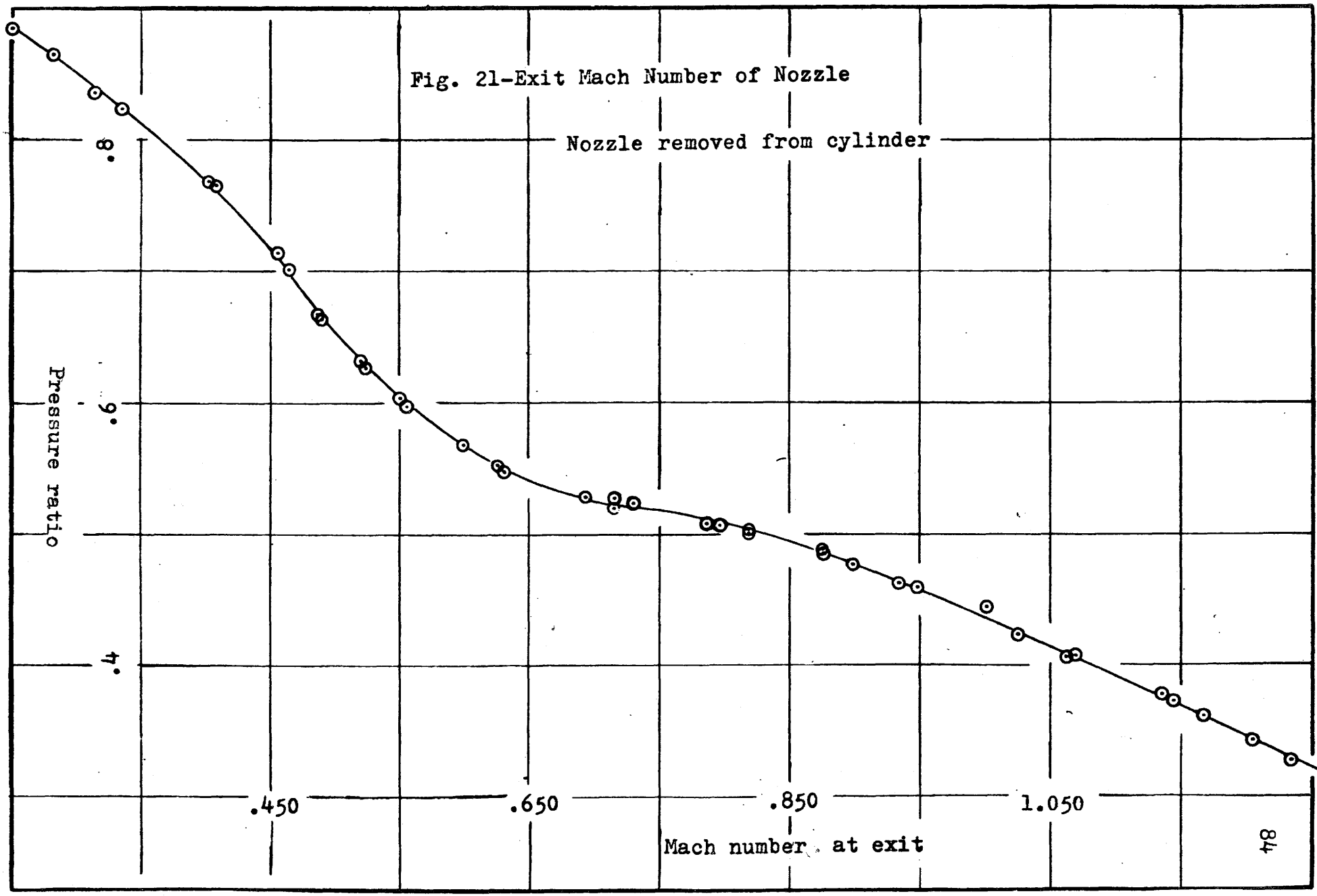
Fig. 21-Exit Mach Number of Nozzle
Nozzle removed from cylinder
Pressure ratio
.8
.6
.4
.450
.650
.850
1.050
Mach number at exit

Fig. 22-Comparison of Pressures and resultant Mach number when using different methods of Static Pressure Measurement

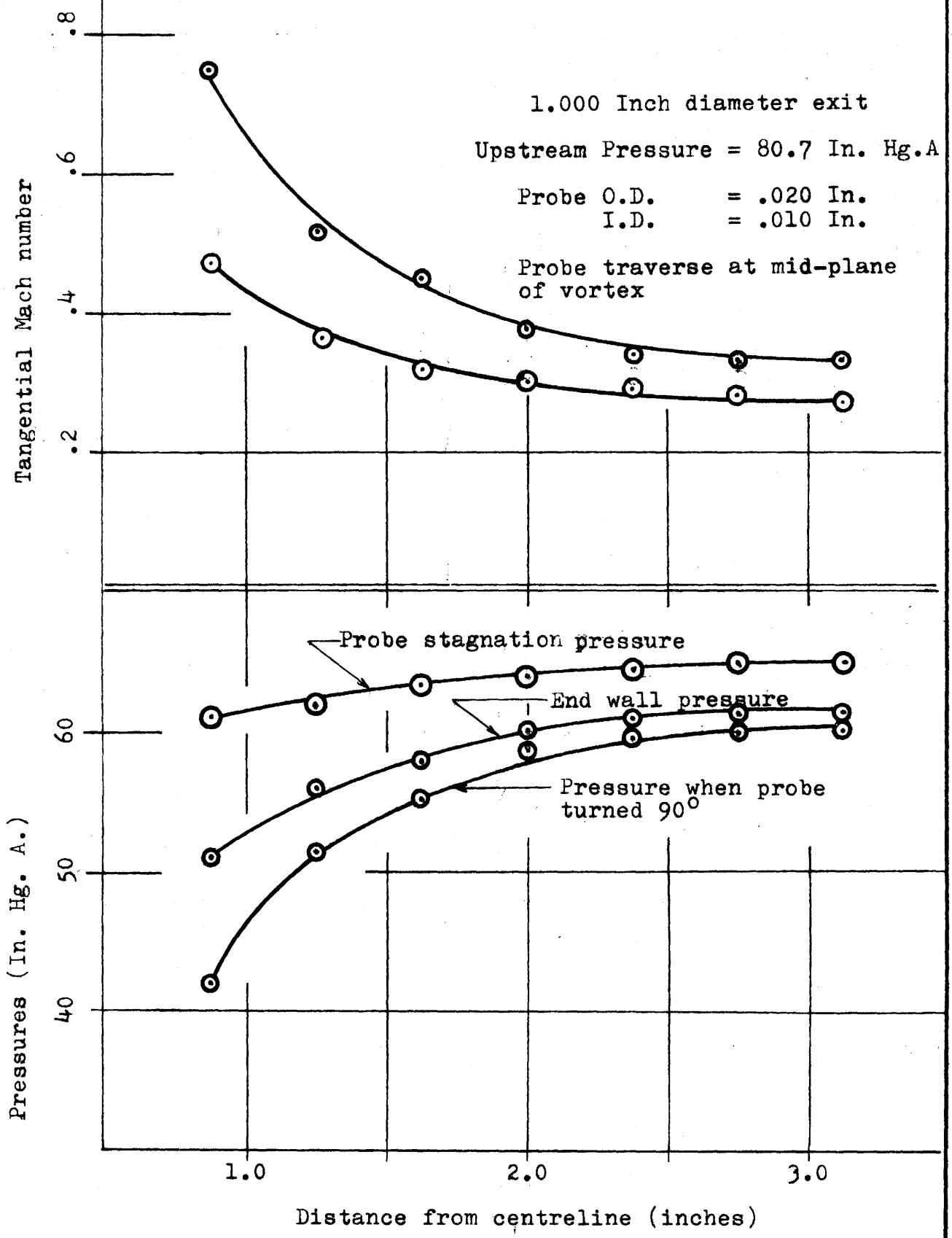

# 10. APPENDIX

## 10.1 Nozzle Testing

Before embarking upon an investigation of the vortex flow itself, it was necessary to know to some degree the performance characteristics of the inlet nozzle. These characteristics were expected to depart from those of conventional supersonic nozzles to a considerable degree, because of the slit type configuration, which resulted in a very small throat dimension in one plane. After considering the problem, it was decided that the following three part experimental investigation would be required;

1. The throat dimensions, being a nominal 6.00 x .0235 inches, would be quite susceptible to large percentage area changes due to distortion of the nozzle blocks under working pressure. It was thought advisable to check the .0235 inch dimension while the nozzle was under pressure.
2. The desirability for two-dimensional flow in the vortex chamber dictated a uniform mass flow and inlet velocity per unit length. As a result the uniformity of flow along the 6 inch nozzle length should be checked.
3. Since the inlet nozzle would probably be operated at pressure ratios other than the design pressure

ratio, its performance under a range of values should be investigated.

Part 1 - Nozzle Dimension Check

A dimension check was performed on the nozzle block on July 22, 1965, using steel feeler gauges, enabling measurement to the closest .001 inch. The results were as follows;

Throat Dimensions

| Upstream Pressure | L.H.S. | Centre | R.H.S. |
|---|---|---|---|
| 0 P.S.I.G. | .022 X 6.000 | .023 X 6.000 | .022 X 6.000 |
| 40 P.S.I.G. | .024 X 6.000 | .026 X 6.000 | .024 X 6.000 |

Upon examination of these results it was decided to structurally strengthen the nozzle block, which was done by doubling the number of through-bolts and of .500 inch diameter polished tool steel spacers.

A new test was carried out on December 11, 1965, and the throat dimensions were again measured using feeler gauges which enabled measurement to the closest .0005 inch. These result are presented below.

Throat Dimensions

| Upstream Pressure | L.H.S. | Centre | R.H.S. |
|---|---|---|---|
| 0 P.S.I.G. | .0235 X 6.000 | .0230 X 6.000 | .0240 X 6.000 |
| 25 P.S.I.G. | .0240 X 6.000 | .0235 X 6.000 | .0250 X 6.000 |
| 50 P.S.I.G. | .0245 X 6.000 | .0240 X 6.000 | .0250 X 6.000 |

Part 2 - Uniformity of Flow along Nozzle

This was experimentally checked by two methods. The first was a total pressure survey taken with a stagnation tube, and the second was by means of Schlieren equipment, which made visible the outlines of the expansions of the supersonic jet after leaving the nozzle exit plane. The results for a test carried out in December, 1965, are presented in the following table;

| | Distance from L.H.S. of Nozzle (inches) | | | | |
|---|---|---|---|---|---|
| | .50 | 1.63 | 2.00 | 5.50 | 4.00 |
| Upstream Pressure P.S.I.G. | 26.0 | 26.0 | 26.0 | 26.0 | 26.0 |
| Stagnation Pressure at exit Plane P.S.I.G. | 24.8 | 24.6 | 24.3 | 25.0 | 24.5 |

Note: "Top" of nozzle block is that side remote from vortex cylinder.

A photograph of the shock structure resulting from the supersonic jet being exhausted to ambient air pressure is shown in Figure 20. Parallelism of the shock diamond structure indicated uniformity in the exiting jet.

Part 3 - Performance under Variable Pressure Ratios.

This test was carried out by supplying the nozzle with different upstream pressures, with the exit flow exhausting to ambient atmospheric pressure. A stagnation probe was located at the exit plane, and the Mach number calculated using the measured stagnation pressure and the ambient barometric pressure as the static pressure, in conjunction with the Rayleigh-Pitot relation for supersonic flow. A calibration curve of Mach number plotted against pressure ratio was then drawn, using approximately 50 experimental values.
The curve is shown on Figure 21.

## 10.2 Einstein and Li's Angular Momentum Relations

The results of Einstein and Li's solution of the Navier-Stokes equations for the conditions as described in Section 6.3.1. are as follows;

$$R'V' = \frac{(A-2)\left(1-e^{-\frac{A}{2}\left(\frac{R'}{R'_o}\right)^2}\right)}{A\left(1-e^{-\frac{A}{2}R'^{(A-2)}_o}\right)-2\left(1-e^{-\frac{A}{2}}\right)}$$

FOR $R' < R'_o$

$A \neq 2$

$$R'V' = \frac{(A-2)\left(1-e^{-\frac{A}{2}}\right)\left(1-R'^{-(A-2)}\right)}{A\left(1-e^{-\frac{A}{2}R'^{(A-2)}_o}\right)-2\left(1-e^{-\frac{A}{2}}\right)} + R'^{-(A-2)}$$

FOR $R' \quad R'_o$

$A \neq 2$

$R' = \dfrac{\text{RADIUS AT ANY POINT}}{\text{RADIUS AT OUTER WALL}}$

$R'_o = \dfrac{\text{RADIUS OF DRAIN HOLE}}{\text{RADIUS AT OUTER WALL}}$

$V' = \dfrac{\text{VELOCITY AT ANY POINT}}{\text{VELOCITY AT OUTER WALL}}$

$A$ = RADIAL REYNOLDS NUMBER

## 10.3 Tangential Velocity-Surface Profile Relation

Einstein and Li (12) used a simple photographic technique when determining the tangential velocities of their water vortex system. The procedure involved will be described in some detail in this section.

The theoretical analysis will first be presented.

If one considers a body of fluid rotating about a vertical axis, in which the fluid forces due to shear stresses can be assumed to be small relative to the gravity and centrifugal forces, the pressure at any point in the liquid can be given by the product of the specific weight of the fluid and the vertical distance from the free surface. When a force balance in a horizontal plane is made, for a small element of fluid in the system, the following relation results;

$$P\nabla a - (P + \frac{\nabla P}{\nabla R})\nabla a = \frac{\nabla a \nabla R \, \delta}{g}(-W^2 R)$$

where $\nabla a$ = cross sectional area of fluid element

$\nabla R$ = length of same element

$P$ = absolute pressure on fluid element

$g$ = acceleration of gravity

$\delta$ = specific weight of fluid

$W$ = angular velocity of fluid at radius considered

$R$ = radial co-ordinate

When simplified the expression becomes

$$\frac{dP}{dR} = \frac{\gamma}{g} W^2 R$$

But the absolute pressure $P = P_0 + \gamma h$

where $P_0$ = ambient pressure at free surface

$h$ = vertical distance from free surface

Therefore $\gamma \frac{dh}{dR} = \gamma \frac{W^2 R}{g}$

But $V_t = W R$

Therefore $\frac{dh}{dR} = \frac{V_t^2}{g R}$

This expression is similar to Einstein and Li's relation, which they derived from a simplified Navier-Stokes approach.

The procedure used in determining $\frac{dh}{dR}$ experimentally is outlined in the following steps;

1. Establish the vortex system and allow the flow to stabilize.
2. Using a camera, preferably having 4 x 5 inch frame size, make an exposure of the surface of the vortex, using a small depth of field, in order to show only the surface profile.

3. Develop and print the negative, enlarging the print to a convenient size.
4. Attach the print to a drafting table, and measure the slope of the surface profile at various radial positions.
5. Figure 15 shows one photograph of a water vortex profile, made with an exit hole diameter of 0.50 inches, and a Radial Reynolds number of 60, while Figure 16 shows the tangential velocities as calculated from the photograph.

It should be noted that these were preliminary investigations only, and the scatter of the results in Figure 15 could be reduced by a refinement of the slope measurement technique.

10.4 Compressible Tangential Velocity Relations by Pengelley.

Pengelley (5) solved the Navier-Stokes equations for the case of a compressible, viscous, two-dimensional vortex, and his derivation will be presented in some detail, as an example of the approach used generally by theoreticians in this area.

The assumptions as made by Pengelley have already been given in Section 6.3.2, and will not be repeated unnecessarily.

He started his derivation by defining the Radial Reynolds number as;

$$A = \frac{m}{2\pi\mu}$$

where $m$ = rate of radial wass flow per unit length

$\mu$ = absolute fluid viscosity

Consider an element of fluid of density $\rho$ and at radius $R$ in a two-dimensional vortex, and from the definition of the Radial Reynolds number, find the radial velocity, $u$

$$u = -\frac{m}{2\pi R \rho}$$

$$= -\frac{A\mu}{R\rho}$$

Differentiating with respect to $R$

$$\frac{du}{dR} = \frac{A\mu}{R^2\rho}\left(1 + \frac{d\rho/dR}{\rho/R}\right)$$

where $u$ = radial velocity, positive for flow outwards from the vortex core.

The Navier-Stokes equations may be written in the following form, for cylindrical co-ordinates.

$$A\left(\frac{dV}{dR} + \frac{V}{R}\right) + \left(R\frac{d^2V}{dR^2} + \left(\frac{dV}{dR} - \frac{V}{R}\right)\right) = 0 \qquad 1$$

$$\frac{dP}{dR} = \left(\frac{\rho V^2}{R}\right)\left(1 + \frac{u^2}{V^2}\left(1 + \frac{d\rho/dR}{\rho/R}\right)\right) \qquad 2$$

where $V$ = tangential velocity

By the definition of circulation for a circular path about the axis of a two-dimensional vortex

$$V = \frac{\Gamma}{2\pi R} \qquad 3$$

By differentiation of (3) and substitution into (1)

$$R \frac{d^2\Gamma}{dR^2} + (A-1)\frac{d\Gamma}{dR} = 0 \qquad 4$$

Integrate (4) twice, and introduce constants $C_1$ and $C_2$, $C_{11}$ and $C_{22}$

$$\Gamma = C_1 - \frac{C_2}{R^{A-2}} \qquad (A \neq 2) \qquad 5$$

$$\Gamma = C_{11} - C_{22} \ln R \qquad (A = 2) \qquad 6$$

Choose $R_o$ so that

$$\left(\frac{d\Gamma}{dR}\right)_o = 2\left(\frac{\Gamma_o}{R_o}\right) \qquad 7$$

This condition implies that the rate of change of angular velocity is zero with respect to radius at Ro and is physically satisfied by solid-body rotation. Applying this condition of equation (7) to equations (5) and (6) gives

$$\frac{V}{Vo} = \frac{R\left(A\left(\frac{Ro}{R}\right)^2 - 2\left(\frac{Ro}{R}\right)^A\right)}{Ro\,(A-2)} \qquad (A \neq 2) \qquad 8$$

$$\frac{V}{Vo} = \frac{R}{Ro}\left(1 - 2\ln\frac{Ro}{R}\right) \qquad (A = 2) \qquad 9$$

The equations (8) and (9) describe the tangential velocity for a compressible viscous two-dimensional vortex. Predictions using the above relations are shown on Figure 17, for values of A of 2.0 and 3.0, and values of Ro as dictated by the geometry of the experimental vortex chamber. As as initial condition for the theoretical prediction, the theoretical velocity was made equal to the experimentally measured value at the wall of the vortex cylinder.

## 10.5 Measured Experimental Data

| Wall Static Pressures (In. Hg. A.) | Total Pressures (In. Hg. A.) | Barometric Pressure (In. Hg. A.) | Exit Diameter (inches) | Upstream Pressure (In. Hg. A.) |
|---|---|---|---|---|
| Distance from centreline (inches)<br>0.75 1.25 1.53 2.00 2.38 2.75 3.13 3.50 | Distance from centreline (inches)<br>.875 1.25 1.63 2.00 2.38 2.75 3.13 3.50 | | | |
| 51.9 56.0 58.8 59.7 60.7 61.0 61.9 62.1 | 60.9 62.2 63.0 63.6 64.4 64.8 65.0 65.4 | 29.70 | 1.000 | 80.7 |
| 41.8 45.0 46.4 47.0 47.6 47.9 48.4 48.6 | 46.9 47.8 48.3 48.7 49.0 49.4 49.8 50.2 | 29.60 | 1.000 | 59.6 |
| 37.9 39.8 40.6 41.0 41.3 41.5 41.9 41.9 | 41.2 42.0 42.2 42.5 42.7 42.9 43.1 43.4 | 29.50 | 1.000 | 49.5 |
| Distance from centreline (inches)<br>1.38 1.75 2.13 2.50 2.88 3.25 | Distance from centreline (inches)<br>1.38 1.75 2.13 2.50 2.88 3.25 | | | |
| 39.5 45.0 48.5 51.0 53.0 55.0 | 52.8 55.5 57.3 58.8 60.4 62.2 | 29.50 | 2.000 | 129.5 |
| 35.5 38.0 41.1 42.5 44.5 46.0 | 41.8 44.0 45.1 45.9 46.8 47.7 | 29.70 | 2.000 | 89.7 |
| 38.0 42.0 45.0 47.5 49.5 51.0 | 46.2 49.3 50.8 51.9 53.0 54.3 | 29.50 | 2.000 | 109.5 |
| 38.0 42.0 45.0 47.5 49.5 51.0 | 47.8 50.0 51.3 52.3 53.8 54.3 | 29.50 | 2.000 | 109.5 |

## 11 REFERENCES


1. M.G. Ranque, Journal de Physique et le Radium, Volume 7, Number 4, 1933.

2. R. Hilsch, "The Use of the Expansion of gases in a Centrifugal Field as a Cooling Process", The Review of Scientific Instruments, Volume 18, Number 2, February, 1947.

3. U.A.F. Williamson, J.A. Tompkins, "Practical Notes on the Design of a Vortex Tube", R.A.E. Technical Note Mechanical Engineering 67, March, 1951.

4. J.P. Hartnett, E.R.G. Eckert, "Experimental Study of the Velocity and Temperature Distribution in a High Velocity Vortex-Type Flow", Heat Transfer and Fluid Mechanics Institute Proceedings, Stanford University, 1956.

5. C.D. Pengelley, "Flow in a Viscous Vortex", Journal of Applied Physics, Volume 28, Number 7, January, 1957.

6. J.J. Keyes, Jr., "An Experimental Study of Gas Dynamics in High Velocity Vortex Flow", Oak Ridge National Laboratory, Oak Ridge, Tennessee, Heat Transfer and Fluid Mechanics Institute Proceedings, Stanford University, 1960.

7. R.G. Deissler, M. Perlmutter, "An Analysis of the Energy Separation in Laminar and Turbulent Compressible Vortex Flows", N.A.C.A. Lewis Flight Propulsion Laboratory, Cleveland, Ohio, Heat Transfer and Fluid Mechanics Institute, Stanford University, 1958.

8. R. Westley, "A Bibliography and Survey of the Vortex Tube", The College of Aeronautics, Cranfield C.O.A. Note 9, March, 1954.

9. W.R. Gambill, N.D. Greene, "Boiling Burnout with Water in Vortex Flow", Chemical Engineering Progress, Volume 54, Number 10, October, 1958.

10. R.R. Long, "A vortex in an Infinite Viscous Fluid", Journal of Fluid Mechanics, June, 1961.

11. R.R. Long, "Vortex Motion in a Viscous Fluid", Journal of Meteology, Volume 15, 1958.

12. H.A. Einstein, H. Li, "Steady Vortex Flow in a Real Fluid", Heat Transfer and Fluid Mechanics Institute Proceedings, Stanford University, 1951.

13. C. du P. Donaldson, R.D. Sullivan, "Behaviour of Solutions of the Navier-Stokes Equations for a Complete Class of the Three-Dimensional Viscous Vortices", Heat Transfer and Fluid Mechanics Institute Proceedings, Stanford University, 1960.

14. C. du P. Donaldson, "The Magnetohydrodynamic Vortex Power Generator: Basic Principles and Practical Problems", Engineering Aspects of M.H.D., Proceedings of 2nd Symposium on Engineering Aspects of M.H.D., Philadelphia, March 9, 10, 1961, Columbia University Press, New York, 1962.

15. C. du P. Donaldson, B.B. Hamel, J.E. McCune, R.S. Snedeker, "Theory of the Magnetohydrodynamic Homopolar Generator", Part 1: Liquid Mediums", Aeronautical Research Associates of Princeton, Report Number 20, September, 1959.

16. J.E. McCune, C. du P. Donaldson, "On the Magneto Gas Dynamics of Compressible Vortices", presented at American Rocket Society Meeting, Los Angeles, May 9-12, 1960.

17. W.S. Lewellen, "Magnetohydrodynamically Driven Vortices", Heat Transfer and Fluid Mechanics Institute Proceedings, Stanford University, 1960.

18. W.S. Lewellen, W.R. Grabowsky, "Nuclear Space Power Systems Using Magnetohydrodynamic Vortices", Americian Rocket Society Journal, May, 1962.

19. M.L. Rosenzweig, W.S. Lewellen, D.H. Ross, "Confined Vortex Flows with Boundary-Layer Interaction", American Institute of Aeronautics and Astronautics Journal, Volume 2, Number 12, December, 1964.

20. M.L. Rosenzweig, D.H. Ross, W.S. Lewellen, "On Secondary Flows in Jet-Driven Vortex Tubes", Journal of the Aerospace Sciences, September, 1962.

21. R.J. Rosa, "Physical Principles of Magnetohydrodynamic Power Generation", The Physics of Fluids, Volume 4, Number 2, February, 1961.

22. L.L. Lengyel, S. Ostrach, "An Analysis of a Vortex-Type Magnetohydrodynamic Induction Generator", N.A.S.A. Technical Note T.N.D. 2006, September, 1963.

23. J.M. Kendall, Jr., "Experimental Study of a Compressible Viscous Vortex", Jet Propulsion Laboratory, Technical Report Number 32-290, June 5, 1962.

24. N. Gregory, J.T. Stuart, W.S. Walker, "On the Stability of Three-Dimensional Boundary Layers with Applications to the Flow due to a Rotating Disc", Proceedings of Royal Society, A,, Volume 248, 1955.

25. A.M. Binnie, J.D. Teare, "Experiments on the Flow of Swirling Water through a Pressure Nozzle and an Open Trumpet", Proceedings of Royal Society, A, September, 1955,

26. W.S. Lewellen, "A solution for Three-Dimensional Vortex Flows with Strong Circulation", Journal of Fluid Mechanics, 1962.

27. G.J. Mullaney, N.R. Dibelius, "Small M.H.D. Power Generator Using Combustion Gases as an Energy Source", American Rocket Society Journal, April, 1961.

28. H. Lamb, Hydrodynamics, Dover Publications, 1932 edition.

29. H.E. Weber, C.H. Marston, "Liquid Metal Vortex M.H.D. Generator", A.S.M.E. Paper Number 63-wa-209, 1963.

30. C. du P. Donaldson, R.S, Snedeker, "Experimental Investigation of the Structure of Vortices in Simple Cylindrical Vortex Chambers", Aeronautical Research Associates of Princeton, Report Number 47, December, 1962.

31. O.L. Anderson, H.D. Taylor, "Theoretical Solutions for the Secondary Flow on the End Wall of a Vortex Tube", United Aircraft Corporation Research Laboratories Report R-2494-1, November, 1961 .

32. D. Wagstaffe, "A Two-Dimensional Supersonic Nozzle for a Vortex Generator", unpublished McMaster University Mechanical Engineering Department Report, April, 1965.

33. H.W. Liepmann, A. Roshko, Elements of Gas Dynamics, John Wiley and Sons, Ine., New York, 1957.

34. L.M. Mack, " The Compressible Viscous Heat-Conducting Vortex", Progess Report Number 20-382, Jet Propulsion Laboratory, California Institute of Technology, May, 1962.

35. J.M. Savino, R.G. Ragsdale, "Some Temperature and Pressure Measurements in Confined Vortex Fields", A.S.M.E. Journal of Heat Transfer, February, 1961.

36. J.P. Holman, G.D. Moore, "An Experimental Study of Vortex Chamber Flow", A.S.M.E. Journal of Basic Engineering, December, 1963.

37. F.S. Simmons, "Recovery Corrections for Butt-Welded, Straight-Wire Thermocouples in High-Velocity, High-Temperature Gas Streams", N.A.C.A. R.M. E54G22a, September,1954.

38. Massachusetts Institute of Technology, Aerodynamic Measurements, Gas Turbine Laboratory, 1953, Eagle Enterprises, Boston,New York.